

Novel Analogues of (*R*)-5-(Methylamino)-5,6-dihydro-4*H*-imidazo[4,5,1-*ij*]quinolin-2(1*H*)-one (Sumanirole) Provide Clues to Dopamine D₂/D₃ Receptor Agonist Selectivity

Mu-Fa Zou,^{†,○} Thomas M. Keck,^{†,▽,○} Vivek Kumar,[†] Prashant Donthamsetti,^{§,¶} Mayako Michino,[‡] Caitlin Burzynski,[†] Catherine Schweppe,[†] Alessandro Bonifazi,[†] R. Benjamin Free,[⊥] David R. Sibley,[⊥] Aaron Janowsky,^{#,||} Lei Shi,^{‡,◆} Jonathan A. Javitch,^{§,¶} and Amy Hauck Newman^{*,†}

[†]Medicinal Chemistry Section and [‡]Computational Chemistry and Molecular Biophysics Unit, Molecular Targets and Medications Discovery Branch, National Institute on Drug Abuse – Intramural Research Program, National Institutes of Health, 333 Cassell Drive, Baltimore, Maryland 21224, United States

[§]Departments of Psychiatry and Pharmacology, Columbia University College of Physicians and Surgeons, New York, New York 10027, United States

[¶]Division of Molecular Therapeutics, New York State Psychiatric Institute, New York, New York 10032, United States

[⊥]Molecular Neuropharmacology Section, National Institute of Neurological Disorders and Stroke, National Institutes of Health, 5625 Fishers Lane, Room 4S-04, Bethesda, Maryland 20892-9405, United States

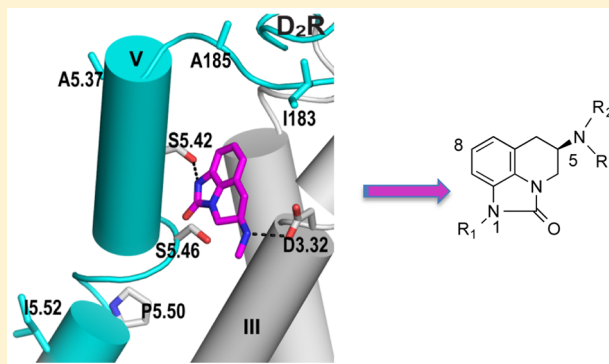
[#]Research & Development Service, Veterans Affairs Portland Health Care System, Portland, Oregon 97239, United States

^{||}Department of Psychiatry and Behavioral Neuroscience, School of Medicine and Methamphetamine Abuse Research Center, Oregon Health & Science University, Portland, Oregon 97239, United States

[◆]Department of Physiology and Biophysics and the Institute for Computational Biomedicine, Weill Medical College of Cornell University, New York, New York 10065, United States

S Supporting Information

ABSTRACT: Novel 1-, 5-, and 8-substituted analogues of sumanirole (**1**), a dopamine D₂/D₃ receptor (D₂R/D₃R) agonist, were synthesized. Binding affinities at both D₂R and D₃R were higher when determined in competition with the agonist radioligand [³H]7-hydroxy-*N,N*-dipropyl-2-aminotetralin (7-OH-DPAT) than with the antagonist radioligand [³H]N-methylpiperone. Although **1** was confirmed as a D₂R-preferential agonist, its selectivity in binding and functional studies was lower than previously reported. All analogues were determined to be D₂R/D₃R agonists in both G_oBRET and mitogenesis functional assays. Loss of efficacy was detected for the *N*-1-substituted analogues at D₃R. In contrast, the *N*-5-alkyl-substituted analogues, and notably the *n*-butyl-arylamides (**22b** and **22c**), all showed improved affinity at D₂R over **1** with neither a loss of efficacy nor an increase in selectivity. Computational modeling provided a structural basis for the D₂R selectivity of **1**, illustrating how subtle differences in the highly homologous orthosteric binding site (OBS) differentially affect D₂R/D₃R affinity and functional efficacy.



INTRODUCTION

Dopamine signaling is mediated by five G protein-coupled receptors (GPCRs). These receptors are divided into two subfamilies on the basis of sequence similarity and pharmacological profiles. D₁-like receptors (D₁R and D₅R) are coupled to G_{α_s} and G_{α_{oif}} that activate adenylyl cyclase-mediated cAMP production, whereas D₂-like receptors (D₂R, D₃R, and D₄R) are coupled to G_{α_{i/o/β}} and inhibit adenylyl cyclase-mediated cAMP production.¹ These receptors also recruit arrestin, which can signal independently of G proteins.¹

The dopamine D₂-like receptor family has long been considered to be an important therapeutic target for the treatment of a variety of neuropsychiatric disorders. Clinically used antipsychotics (e.g., haloperidol) are well-known D₂-like receptor antagonists; this includes second-generation agents that have reduced extrapyramidal side effects and are thus termed “atypical” antipsychotics (e.g., quetiapine, olanzapine,

Received: October 14, 2015

Published: April 1, 2016

and clozapine).^{2–4} Further, D₂-like receptor agonists (e.g., pergolide, bromocriptine, talipexole, pramipexole, ropinirole, and cabergoline) have been used to treat symptoms of Parkinson's disease as well as associated dyskinesias and have a variety of potential neuroprotective properties.⁵

Nevertheless, medications that target D₂-like receptors are associated with adverse side effects that reduce quality of life and medication compliance. This may in part be due to their inability to distinguish between D₂-like receptor subtypes, especially between the highly homologous D₂R and D₃R, which are expressed differentially in the brain and mediate distinct physiological and behavioral processes. D₂Rs are highly expressed in the dorsal striatum and are also found at significant levels in substantia nigra, ventral tegmental area, nucleus accumbens, olfactory tubercle, hypothalamus, amygdala, cortex, and hippocampus.^{1,6} D₂Rs contribute to the control of locomotion, learning, memory, and the rewarding response to addictive drugs.⁷ In contrast, D₃Rs are primarily expressed in the ventral striatum, including the nucleus accumbens,⁶ and are a target of interest in addiction pharmacotherapy.^{8–14}

The development of subtype-selective ligands at these D₂-like receptors has been challenging. Although substantial effort has led to the development of D₃R- and D₄R-selective ligands,^{9,15–17} significantly less progress has been made toward the development of D₂R-selective compounds. Novel D₂R-selective ligands can be useful as tools to probe the roles of D₂-like receptor subtypes in vivo and could potentially lead to new pharmacotherapeutics for the treatment of a variety of disorders (e.g., antagonists for schizophrenia, partial or full agonists for Parkinson's disease, hyperprolactinemia, and restless legs syndrome).

Sumanirole ((*R*)-5,6-dihydro-5-(methylamino)-4*H*-imidazo[4,5,1-*ij*]quinolin-2(1*H*)-one (*Z*)-2-butenedioate, **1**, U-95666E, PNU-95666E; Figure 1) was reported previously to be a D₂R-

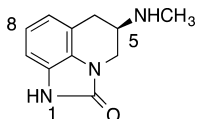


Figure 1. Structure of sumanirole (**1**).

selective metabolite of (*R*)-5,6-dihydro-*N,N*-dimethyl-4*H*-imidazo[4,5,1-*ij*]quinolin-5-amine,^{18,19} one compound in a series of imidazoquinolinones with varying dopaminergic and serotonergic activities.^{20,21} A detailed pharmacological analysis of **1** described this compound as a dopaminergic agonist with >200-fold higher affinity for D₂R than for D₃R based on radioligand binding studies.²² As such, **1** has been used in a variety of studies seeking to disentangle the roles of D₂R and D₃R signaling in vivo (e.g., see refs 23–26). Compound **1** was evaluated in clinical trials for the treatment of Parkinson's disease and restless legs syndrome but is not clinically approved.^{27–31}

The orthosteric binding site (OBS)—the site in which dopamine binds to induce receptor signaling—is virtually identical in D₂R and D₃R.³² It is unclear how **1**, which presumably binds in the OBS, is highly selective for D₂R over D₃R. Therefore, the goal of this study is to further examine the binding profile of **1** and to begin to elucidate the molecular determinants that confer subtype selectivity through chemical modification of the parent molecule at positions 1, 5, and 8.

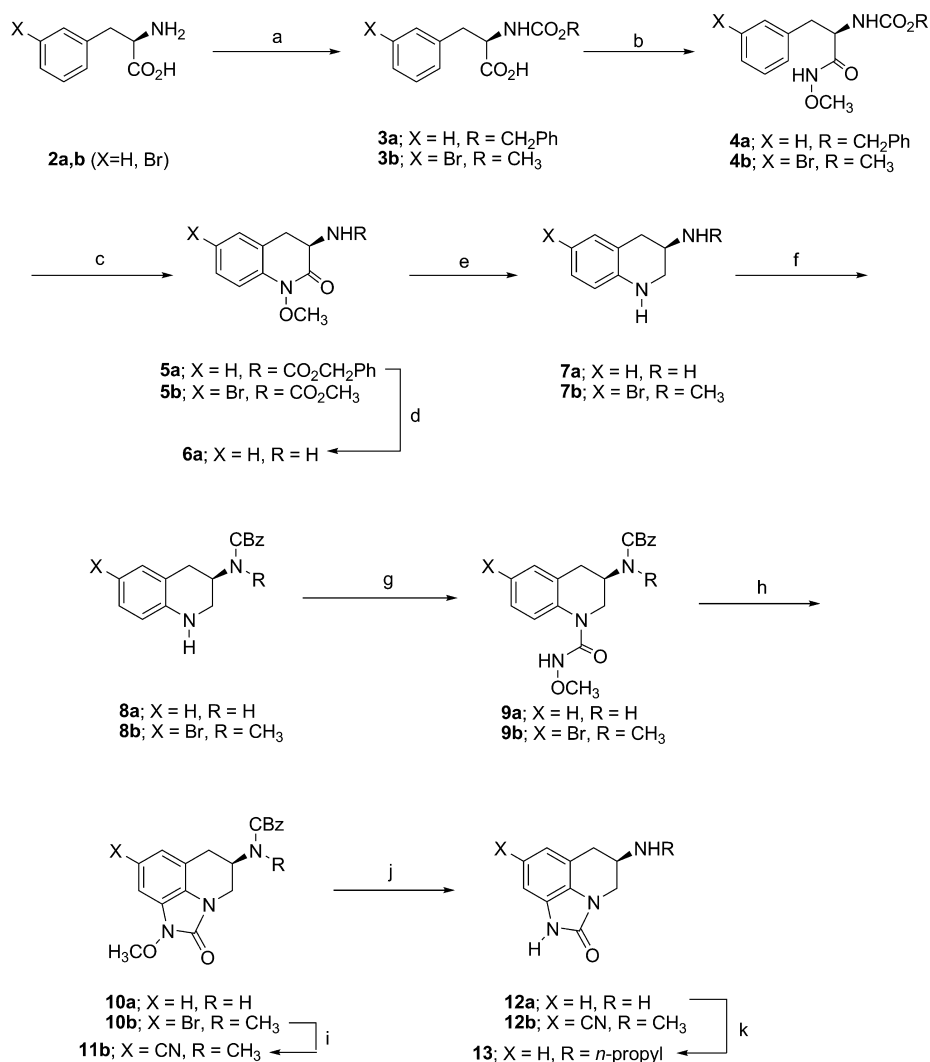
Highly D₃R-selective compounds have been discovered using a “bivalent” design, which includes a high-affinity primary pharmacophore (PP), such as 4-phenylpiperazine, connected to an extended aryl amide functional group that occupies a secondary receptor binding pocket (SBP) to enhance subtype selectivity.^{32–34} Previously, we used a “synthon” approach to define the role of the primary and secondary pharmacophores (PP and SP, respectively) in D₃R subtype selectivity and efficacy.^{33,34} In this study, we take a similar approach using **1** as the PP, adding structural complexity through alkylation at the 1 and *N*-5 positions, adding a CN to the 8 position, and creating the first bivalent analogues of **1** by extending an aryl amide from its *N*-5 position with a butyl linking chain.

Synthetic strategies for **1** have been described previously.^{18,35–40} In the present study, we extend this strategy to a series of analogues for which we develop structure–activity relationships (SAR) for both binding and receptor activation at D₂R and D₃R comparatively. We identify fully efficacious analogues and D₂R-preferential ligands with extended aryl amide pharmacophores. Finally, using molecular modeling and simulations with **1** and selected analogues, we begin to explore the molecular interactions between these ligands at D₂R and D₃R to investigate the structural basis of D₂R over D₃R selectivity and efficacy.

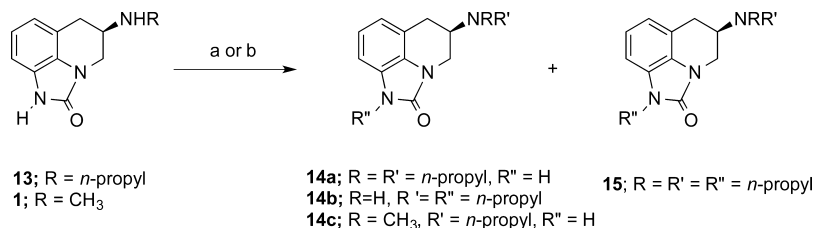
CHEMISTRY

For the synthesis of **12a**, **12b**, and **13**, we adopted a strategy similar to the one used for the synthesis of compound **1**³³ and depicted in Scheme 1. *D*-Phenylalanine (**2a**) or its 3-Br (**2b**) analogue was reacted with methyl chloroformate or benzyl chloroformate to form **3a** and **3b**, respectively, which were then coupled with methoxyamine in the presence of 1-(3-(dimethylamino)propyl)-3-ethylcarbodiimide (EDC) to give **4a** and **4b**, respectively. Cyclization resulted by treating **4a** and **4b** with bis(trifluoroacetoxy)iodobenzene to afford **5a** and **5b** in good yields. Deprotection of **5a** was implemented with Pd/C-catalyzed hydrogenolysis to afford **6a**, which was reduced with borane to give **7a**.²⁰ It was observed that **6a** did not dissolve well in THF; thus, the reaction times were longer for **6a** for reduction completion (5 days). Selective protection of the basic amines in **7a** and **7b** were effected by treating with *N*-(benzyloxycarbonyl)succinimide at –40 °C to afford **8a** and **8b**, which were treated with phosgene, followed by methoxyamine, to produce **9a** and **9b**, respectively. Compounds **9a** and **9b** were reacted with bis(trifluoroacetoxy)iodobenzene to provide the tricyclic products **10a** and **10b**. Removal of the carbobenzyloxy (CBz) protecting group and cleavage of the *N*-methoxy group in **10a** by means of hydrogenolysis over Pd(OH)₂/C (Pearlman's catalyst) gave product **12a**.²⁰ Conversion of the 3-Br in **10b** to 3-CN was conducted by Pd-catalyzed cross-coupling of **10b** with Zn(CN)₂ to give **11b**, which was then transformed to the final product **12b** by hydrogenolysis over Pearlman's catalyst. Reductive amination of **12a** with propionaldehyde and sodium triacetoxyborohydride afforded **13**.²⁰

Compounds **14a**, **14b**, and **15** were prepared from **13**. For **14a**, reaction of **13** with benzylchloroformate primarily and unexpectedly protected the 1-position amide nitrogen rather than the secondary amine. Reaction with 1-bromopropane (Scheme 2) gave the *N,N*-dipropylamine intermediate, which upon hydrogenolysis of the CBz protecting group gave **14a**. ¹H NMR and optical rotation data corresponded with this previously reported structure.²⁰ Direct alkylation of **13** in

Scheme 1. Synthesis of Analogues 12a, 12b, and 13^a

^aReagents and conditions: (a) ClCO₂CH₃ or CbzCl, aq NaOH, THF/H₂O, 2 h; (b) CH₃ONH₂, EDC, CH₂Cl₂, 24 h; (c) PhI(O₂CCF₃)₂, CF₃CO₂H, CH₂Cl₂, 0 °C, 1 h; (d) H₂ (50 psi), Pd/C (10%), EtOH; (e) BH₃·Me₂S, THF, reflux; (f) *N*-(benzyloxycarbonyloxy)succinimide, toluene, -40 °C, 30 min; (g) i. COCl₂, Et₃N, THF; ii. CH₃ONH₂; (h) PhI(O₂CCF₃)₂, CHCl₃, -5 °C; (i) Zn(CN)₂, Pd(PPh₃)₄, DMF; (j) H₂ (50 psi), Pd(OH)₂/C, EtOH; (k) CH₃CH₂CHO, NaBH(OAc)₃, THF.

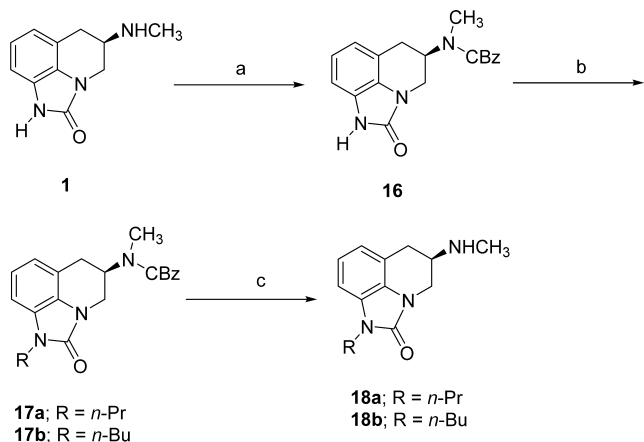
Scheme 2. Synthesis of Analogues 14a–c and 15^a

^aReagents and conditions: (a) i. Cbz-Cl, Et₃N, THF; ii. *n*-PrBr, K₂CO₃, DMF, heat; iii. H₂, 10% Pd/C, EtOH; (b) *n*-PrBr, K₂CO₃, DMF, heat.

DMF with K₂CO₃ gave a mixture of **14b** and **15**. The ratio of the two products (**14b**:**15**) depended on the reaction temperature, reaction time, and the ratio of **13** to 1-bromopropane. We found only product **14b** was formed if the reaction temperature was kept at 40 °C or below, but the reaction was slow. The yield of product **15** could be improved by increasing the ratio of 1-bromopropane to **13**, increasing the temperature, and prolonging the reaction time (details in

Experimental Methods). Compound **14c** was prepared using the same alkylation procedure as described for **14b**, starting with compound **1**.

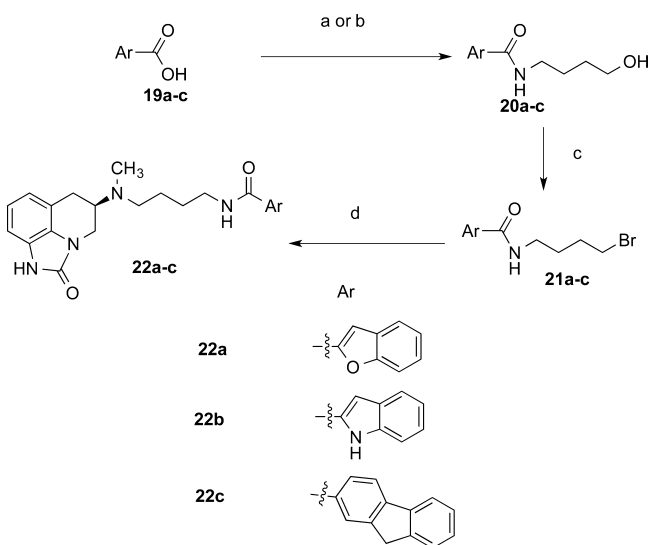
Compounds **18a** and **18b** were synthesized according to Scheme 3. Protection of the basic nitrogen on **1** with the CBz group using *N*-(benzyloxycarbonyloxy)succinimide afforded intermediate **16**, which was treated with either NaH or K₂CO₃ followed by reaction with 1-bromopropane or 1-

Scheme 3. Synthesis of Analogues 18a and 18b^a

^aReagents and conditions: (a) *N*-(benzyloxycarbonyloxy)succinimide, THF, -40°C to rt, 16 h; (b) NaH or K_2CO_3 , RBr, THF, rt; (c) H_2 (50 psi), Pd/C (10%), EtOH, 5 h.

bromobutane to give 17a and 17b, respectively. Deprotection of the CBz group on 17a and 17b by Pd/C-catalyzed hydrogenolysis provided products 18a and 18b, respectively.

Scheme 4 outlines the synthetic strategy used for the synthesis of the aryl amide butyl-substituted derivatives 22a–c.

Scheme 4. Synthesis of Analogues 22a–c^a

^aReagents and conditions: (a) i. SOCl_2 ; ii. $\text{NH}_2(\text{CH}_2)_4\text{OH}$, 0°C to rt; (b) i. CDI, THF, rt; ii. $\text{NH}_2(\text{CH}_2)_4\text{OH}$, 0°C to rt; (c) Ph_3P , CBr_4 , CH_3CN ; (d) 1, K_2CO_3 , DMF, $60\text{--}65^{\circ}\text{C}$, 3 h.

Compounds 20a, 20b, 21a, and 21b were synthesized according to the earlier published procedure.⁴¹ Compound 20c was synthesized via the acid chloride and was converted to 21c with Ph_3P and CBr_4 . Coupling of 1 with 21a–c under basic conditions afforded the desired compounds 22a–c.

RESULTS AND DISCUSSION

D₂R and D₃R Binding and Functional Data. Compound 1 was reported previously to be a highly selective D₂R agonist²² and thus should bind preferentially to the high affinity (active) conformation of D₂R. We determined the dissociation constant

(K_i) values of 1 and its analogues as well as the prototypical D₂-like agonists dopamine, 7-OH-DPAT, and quinpirole using both agonist and antagonist tracer ligands (Table 1). Not surprisingly, the absolute K_i values for these agonists at both D₂R and D₃R were lower (i.e., higher affinities) when determined in competition with the agonist radioligand [³H]7-OH-DPAT compared to the antagonist radioligand [³H]N-methylspiperone. This is consistent with previous results demonstrating substantial probe sensitivity with dopamine receptor agonists, which more readily compete with agonist radioligands than antagonist radioligands.⁴²

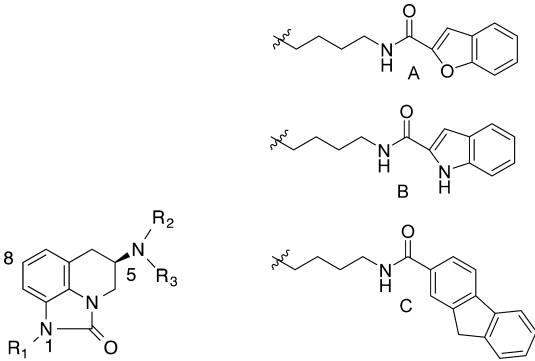
Compound 1 was previously reported to be 215-fold selective for D₂R over D₃R.²² Notably, the previous analysis relied upon an agonist radiotracer at D₂R ([³H]U-86170)⁴² ([³H]14a) but an antagonist radiotracer at D₃R ([³H]spiperone), thereby potentially biasing the selectivity toward D₂R. We discovered that when using the antagonist [³H]N-methylspiperone as the radioligand, 1 displayed very low affinity for D₂R and D₃R ($K_i \geq 16$ and $6.3 \mu\text{M}$, respectively) and was slightly D₃R-selective (~ 2.5 -fold). When the agonist [³H]7-OH-DPAT was used as the radiotracer, 1 displayed high affinity at D₂R ($K_i = 17.1 \text{ nM}$), a slightly higher K_i value than reported ($K_i \approx 9 \text{ nM}$) using [³H]14a).^{18,22} In our assay, using [³H]7-OH-DPAT as the radiotracer, the affinity of 1 for D₃R was higher ($K_i = 546 \text{ nM}$) than previously reported ($K_i = 1940 \text{ nM}$ using [³H]spiperone).²² Thus, using [³H]7-OH-DPAT at both receptors, we determined 1 to be 32-fold D₂R-selective over D₃R rather than >200-fold as previously reported.²²

Like the parent compound 1, its analogues displayed binding affinities at D₂R that were 28- to 955-fold higher when using [³H]7-OH-DPAT as compared to [³H]N-methylspiperone as the competitive radioligand. Binding to D₃R exhibited the same probe-dependent pattern but with a smaller magnitude difference in calculated K_i , increasing <40-fold when using [³H]7-OH-DPAT as compared to [³H]N-methylspiperone as the competitive radioligand.

Because 1 and its analogues appeared to be agonists at both D₂R and D₃R based on their binding profiles—i.e., higher affinity in competition with agonist as compared to antagonist radiotracers—we focused on structure–activity relationships (SAR) at D₂R and D₃R using the agonist [³H]7-OH-DPAT as the tracer ligand. Removing the *N*-CH₃ (12a) reduced affinities at both D₂R and D₃R by ~ 6 -fold. The addition of an 8-CN group (12b) nearly abolished affinity at D₂R, so further modification at this position was not pursued.

By replacing the *N*-5-CH₃ group in 1 with an *n*-propyl group (13), both D₂R and D₃R binding affinities improved ($K_i = 2.78$ and 25.5 nM , respectively). Whereas the *N,N*-di-*n*-propyl analogue, 14a, demonstrated similar affinity at D₃R to 13, the D₂R affinity was decreased ~ 4 -fold. The *n*-propylation at position 1 (14b) had little effect on D₂R and D₃R binding affinities, and addition of the *N*-5-*n*-propyl to 1 (14c) maintained a similar D₂R affinity ($K_i = 12.5 \text{ nM}$) but led to a small increase in D₃R affinity, rendering this analogue less D₂R selective (~ 8 -fold) than the parent compound (32-fold).

Global *N*-*n*-propyl substitutions at positions 1 and 5 (15) uniformly improved both D₂R and D₃R binding affinities. Of note, this analogue displayed similarly high affinities ($K_i \sim 3 \text{ nM}$) for D₂R and D₃R. Alkylation at the position 1 imidazopyridine nitrogen (18a, b) did not affect binding affinities at D₂R as compared to the parent molecule. However, D₃R affinities improved ~ 3 – 5 -fold. Addition of the butyl-linked arylamide

Table 1. In Vitro Radioligand Competition Binding at hD₂R and hD₃R


compound	structure	cLogP	[³ H]N-methylspiperone competition ^a			[³ H]7-OH-DPAT competition ^a		
			hD ₂ R		hD ₃ R	hD ₂ R		hD ₃ R
			K _i ± SEM (nM)	K _i ± SEM (nM)	D ₃ /D ₂	K _i ± SEM (nM)	K _i ± SEM (nM)	D ₃ /D ₂
dopamine		0.17	3,690 ± 845	293 ± 92.0	0.08	8.73 ± 1.11	7.58 ± 2.12	0.87
7-OH-DPAT		4.0	143 ± 15.2	1.75 ± 0.355	0.01	2.27 ± 0.211	1.49 ± 0.393	0.66
quinpirole		0.27	2,950 ± 410	29.3 ± 2.66	0.01	5.56 ± 0.396	8.01 ± 1.75	1.4
1	R ₁ =R ₂ =H, R ₃ =CH ₃	1.3	16,300 ± 2,930	6,330 ± 653	0.39	17.1 ± 2.03	546 ± 142	32
12a^c	R ₁ =R ₂ =H, R ₃ =H	1.0	12,100 ± 789	11,800 ± 3,660	0.98	114 ± 18.5	3,390 ± 724	30
12b	R ₁ =R ₂ =H, R ₃ =CH ₃ , 8-CN	1.2	N.T. ^b	27,200 ± 2,600		5,120 ± 307	N.T. ^b	
13^c	R ₁ =R ₂ =H, R ₃ =n-Pr	2.4	2,430 ± 468	410 ± 41.9	0.17	2.78 ± 0.273	25.5 ± 2.59	9.2
14a^c	R ₁ =H, R ₂ =R ₃ =n-Pr	4.0	N.T. ^b	N.T. ^b		11.4 ± 1.05	27.1 ± 2.33	2.4
14b	R ₁ =R ₂ =n-Pr, R ₃ =H		868 ± 111	47.9 ± 9.39	0.06	8.08 ± 2.28	21.7 ± 1.28	2.7
14c	R ₁ =H, R ₂ =n-Pr, R ₃ =CH ₃	2.9	1,180 ± 312	290 ± 49.8	0.25	12.5 ± 2.54	104 ± 9.24	8.3
15	R ₁ =R ₂ =R ₃ =n-Pr	5.1	146 ± 1.48	6.05 ± 1.61	0.04	2.59 ± 0.177	3.39 ± 0.313	1.3
18a	R ₁ =n-Pr, R ₂ =H, R ₃ =CH ₃	2.4	751 ± 27.8	187 ± 14.0	0.25	13.2 ± 3.26	99.5 ± 1.19	7.5
18b	R ₁ =n-Bu, R ₂ =H, R ₃ =CH ₃	3.0	361 ± 38.9	10.3 ± 2.40	0.03	12.8 ± 2.39	142 ± 8.65	11
22a	R ₁ =H, R ₂ =A, R ₃ =CH ₃	3.7	14,700 ± 4,890	2,610 ± 588	0.18	15.5 ± 1.32	256 ± 51.5	17
22b	R ₁ =H, R ₂ =B, R ₃ =CH ₃	5.0	4,230 ± 1,680	337 ± 19.8	0.08	5.78 ± 0.418	76.9 ± 6.39	13
22c	R ₁ =H, R ₂ =C, R ₃ =CH ₃	3.7	3,700 ± 777	1,090 ± 208	0.29	5.47 ± 1.11	12.5 ± 3.13	2.3

^aEach K_i value represents data from at least three independent experiments with each performed in triplicate. Binding assays are described in detail in the [Experimental Methods](#). ^bN.T. = not tested. ^cCompound previously reported by Moon et al.²⁰ ^dDetermined with ChemBioDraw Ultra 14.0.

Table 2. In Vitro Agonist Activity at hD₂R and hD₃R

compound	hD ₂ R G _o BRET		hD ₃ R G _o BRET		hD ₂ R mitogenesis		hD ₃ R mitogenesis	
	EC ₅₀ ± SEM (nM)	% DA max ± SEM	EC ₅₀ ± SEM (nM)	% DA max ± SEM	EC ₅₀ ± SEM (nM)	% DA max ± SEM	EC ₅₀ ± SEM (nM)	% DA max ± SEM
dopamine	5.0 ± 1.4	100	1.8 ± 0.2	100	7.7 ± 0.8	100 ± 3.0	2.7 ± 0.7	106 ± 2.1
quinpirole	N.T. ^b	N.T. ^b	N.T. ^b	N.T. ^b	8.2 ± 1.1	99 ± 1.2	3.3 ± 0.7	102 ± 2.9
1	60.1 ± 13	96.9 ± 2.5	186 ± 49	101 ± 6.0	64.7 ± 2.6	100 ± 2.2	669 ± 88	157 ± 1.6
12a^c	697 ± 190	92.0 ± 2.3	1890 ± 450	85.2 ± 5.9	684 ± 7.2	95.3 ± 2.6	3400 ± 480	139 ± 5.8
13^c	16.0 ± 3.6	101 ± 2.7	18.3 ± 4.4	94.5 ± 3.3	1.0 ± 0.10	97.3 ± 5.8	0.81 ± 0.05	107 ± 3.0
14a^c	2.53 ± 0.58	109 ± 6.3	21.8 ± 2.9	86.9 ± 2.6	N.T. ^b	N.T. ^b	N.T. ^b	N.T. ^b
14b	68.0 ± 3.1	85.6 ± 5.0	1423 ± 4.4	64.5 ± 5.2	13.0 ± 0.5	92.1 ± 4.2	56.1 ± 7.2	52.0 ± 4.1
14c	29.0 ± 6.6	80.0 ± 3.6	30.7 ± 6.4	58.6 ± 2.2	18.1 ± 0.5	91.6 ± 5.0	148 ± 4.0	85.4 ± 9.2
15	33.9 ± 8.2	88.2 ± 3.5	51.9 ± 7.9	53.5 ± 8.0	13.7 ± 3.6	108 ± 2.7	3.7 ± 1.4	47.0 ± 7.3
18a	38.7 ± 22	95.8 ± 3.9	53.7 ± 18	74.5 ± 5.1	549 ± 36	92.0 ± 6.4	178 ± 38	58.0 ± 3.5
18b	30.5 ± 14	84.8 ± 7.2	25.6 ± 7.5	40.4 ± 8.3	83.0 ± 18	56.0 ± 3.6	22.0 ± 4	28.0 ± 1.6
22a	43.3 ± 11	103 ± 3.0	115 ± 24	88.1 ± 4.2	19.5 ± 3.5	96.4 ± 4.9	19.6 ± 6.1	97.2 ± 2.8
22b	22.7 ± 5.4	107 ± 2.5	94.3 ± 23	86.9 ± 2.6	27.7 ± 3.5	106 ± 2.7	53.0 ± 16	103 ± 4.6
22c	109 ± 18	104 ± 3.2	125 ± 43	95.3 ± 3.1	102 ± 3.7	90.1 ± 9.9	11.9 ± 4.1	105 ± 2.9

^aEach EC₅₀ value represents data from at least three independent experiments. Functional assays are described in detail in the [Experimental Methods](#). ^bN.T. = not tested. ^cCompound previously reported by Moon et al.²⁰ DA = dopamine.

(22a–c), used frequently in the 4-phenylpiperazine class of D₃R-selective antagonists/partial agonists, resulted in D₂R-selective agonists with high affinities (K_i = 5–15 nM). The discovery that all three of these analogues retained high binding

affinities and D₂R selectivities suggests that these molecules may not access the secondary binding pocket in the same way that the 4-phenylpiperazine-based D₃R-selective antagonists/partial agonists do^{12,33,43} and implies an important role of the

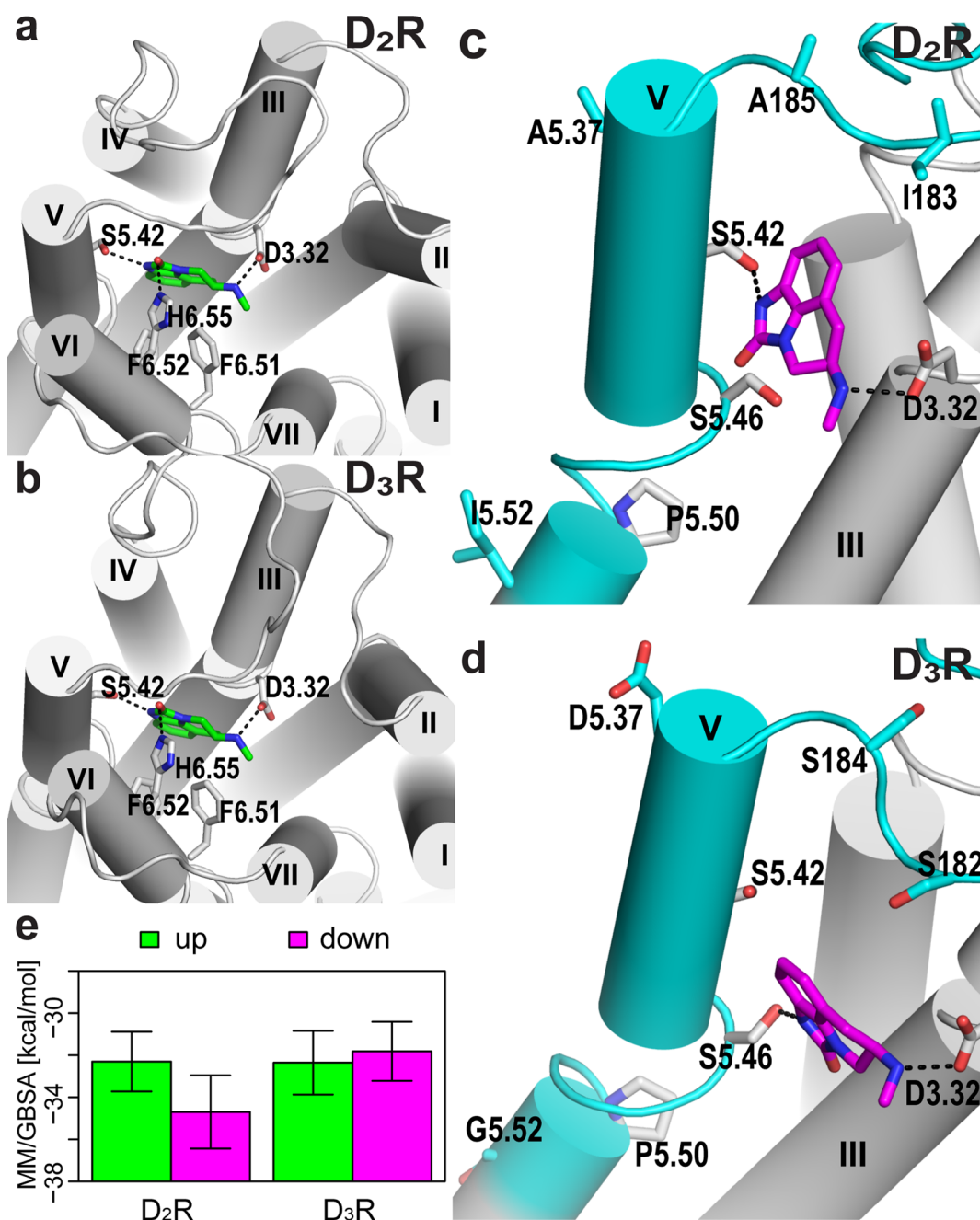


Figure 2. Predicted binding modes of **1** in D₂R and D₃R. (a–d) The “up” poses of **1** in D₂R (a) and D₃R (b) converged, forming ligand–receptor interactions with Asp^{3.32}, Ser^{5.42}, Phe^{6.51}, Phe^{6.52}, and His^{6.55}, whereas the “down” poses in D₂R (c) and D₃R (d) showed divergent interactions. The ligand is shown as sticks in green for the “up” pose and in magenta for the “down” pose. The different conformations of the EL2 and the N-terminal segment of TMS between D₂R and D₃R (cyan) likely result from the divergent amino acid residues within this region (cyan sticks) and may contribute to the differential binding modes in D₂R and D₃R. TMs 6 and 7 are not shown for clarity. (e) The average and standard deviation of MM/GBSA receptor–ligand binding energy values from the last 60 ns of MD trajectories are shown as a barplot for the “up” and “down” poses in D₂R and D₃R. In D₂R, the “down” pose has lower binding energy values than the “up” pose, whereas in D₃R, the reverse preference is observed. The “down” pose in D₂R has lower binding energy values than the “up” pose in D₃R, consistent with the selectivity of **1** for D₂R over D₃R.

5,6-dihydro-4*H*-imidazo[4,5,1-*ij*]quinolin-2(1*H*)-one PP in positioning the rest of the molecule in D₂R.

To evaluate the functional activity of **1** and its analogues at D₂R or D₃R, these compounds were evaluated in two different in vitro functional assays (Table 2). A bioluminescence resonance energy transfer (BRET)-based assay was used to measure agonist-induced activation of G α_{oA} by either D₂R or D₃R. In this assay, receptor activation leads to the separation of G α_{oA} -91-Rluc8 and complemented mVenus-G $\beta_1\gamma_2$ and a

reduction in BRET.³³ In addition, a mitogenesis assay was used to characterize dose–response curves for receptor-mediated incorporation of [³H]thymidine in cells expressing the recombinant D₂R or D₃R.

Overall, **1** and its analogues displayed agonist profiles at D₂R and D₃R in both the G_o BRET and mitogenesis assays as compared to standard D₂-like agonists dopamine and quinpirole. As expected for compounds with high efficacy, G_o BRET and mitogenesis EC₅₀ values were more similar to K_i

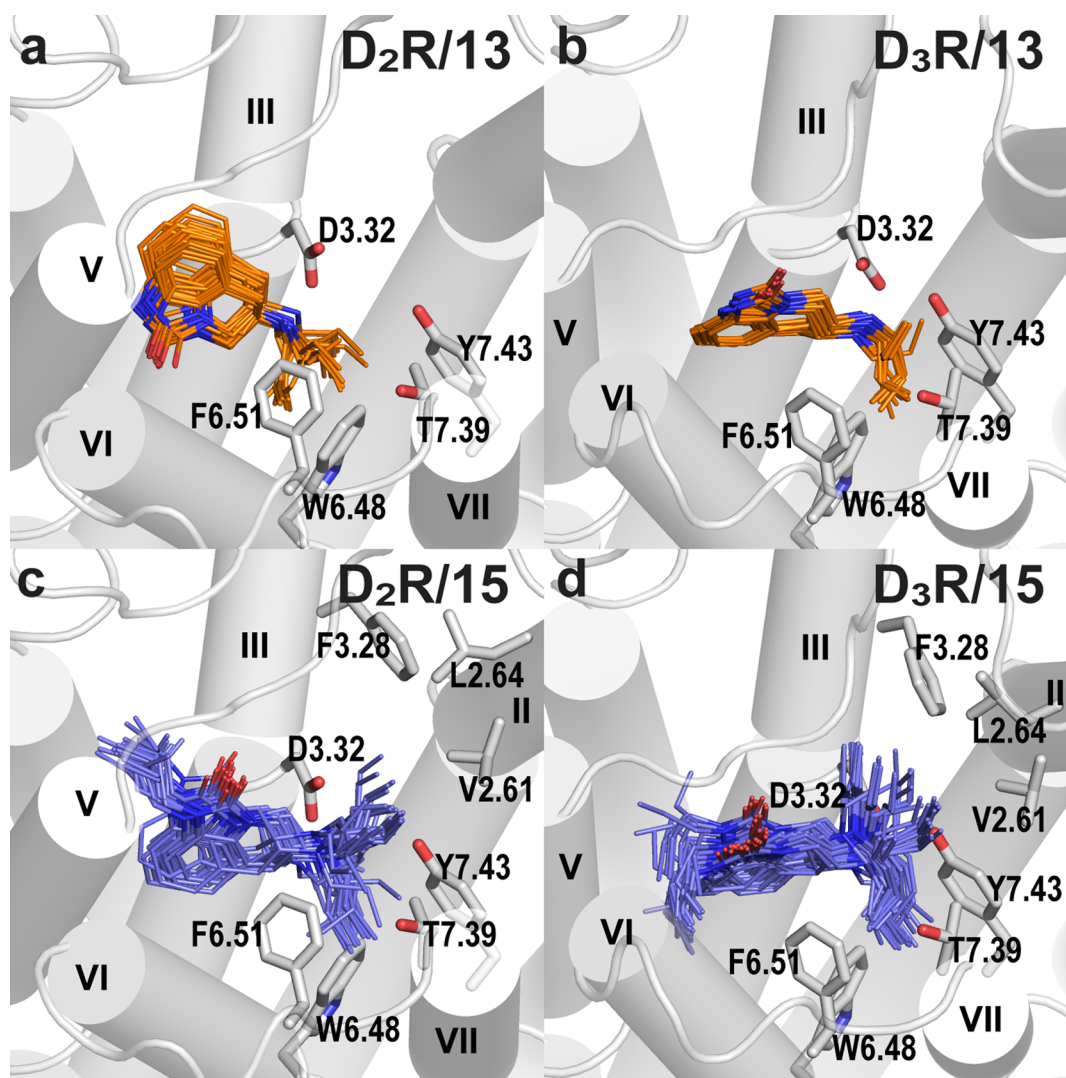


Figure 3. Predicted binding modes of analogues 13 and 15 in D₂R and D₃R. For each compound, the largest cluster of poses is shown. Compound 13 (orange) binds with similar orientational preference as 1 in both D₂R (a) and D₃R (b), whereas 15 (slate blue) reverses to the “up” pose in D₂R (c) as in D₃R (d). The *n*-propyl group of 13 interacts with the Ptm67 pocket residues Trp^{6.48}, Phe^{6.51}, Thr^{7.39}, and Tyr^{7.43}. The additional *n*-propyl group of 15 interacts with the Ptm23 pocket residues Val^{2.61}, Leu^{2.64}, and Phe^{3.28}.

values calculated in competition with the agonist radioligand [³H]7-OH-DPAT than to *K_i* values calculated in competition with the antagonist radioligand [³H]*N*-methylspiperone. These results are more pronounced with D₂R (compared to D₃R), an observation consistent with the substantial relative difference between the high- and low-affinity receptor populations of D₂R and D₃R.⁴⁴ Agonist binding at D₂R can be robustly inhibited by nonhydrolyzable analogues of GTP, dramatically shifting apparent *K_i* values. In contrast, D₃R agonist binding is relatively insensitive to nonhydrolyzable GTP analogues, maintaining substantial high-affinity binding in the absence of efficient G protein signaling.^{45–47} The partial retention of high-affinity binding at D₃R in conditions that favor low-affinity binding, i.e., in the [³H]*N*-methylspiperone binding assay, is a likely explanation for the less dramatic difference between [³H]7-OH-DPAT-derived and [³H]*N*-methylspiperone-derived *K_i* values at D₃R in comparison to the very large differences seen at D₂R.

In an assay of receptor-activated mitogenesis, McCall et al. (2005) reported an EC₅₀ of 4.6 nM at D₂R for 1, but no activity was observed in a D₃R-mediated mitogenesis assay when tested

using concentrations up to 1 μM, although the data were not shown.²² In contrast, we report that 1 is a fully efficacious agonist in mitogenesis assays at both D₂R and D₃R (EC₅₀ = 65 and 669 nM, respectively; Table 2). Overall, our data for both G_o BRET and mitogenesis suggest that 1 is a full agonist at both D₂R and D₃R and only modestly (3–10-fold) D₂R-selective over D₃R in these cell-based functional assays (Table 2). It is notable that our binding and functional studies agree that, although 1 is certainly a *preferential* agonist for D₂R over D₃R, the degree of subtype selectivity may be more modest than previously suggested.

In addition, D₂R binding selectivity over D₃R for this series of ligands is more pronounced than D₂R selectivity in the functional assays. The most potent and fully efficacious D₂R agonist in this set was 14a (EC₅₀ = 2.53 nM, Table 2). Curiously, compounds 14b, 15, and 18a, which have an *n*-propyl group at the 1-position, each show modest but significantly decreased efficacy at D₃R compared to D₂R, which may suggest functional separability between subtypes. This decrease in efficacy was even more dramatic (40.4% at D₃R vs 84.8% at D₂R, Table 2) with *n*-butyl-substituted 18b.

The analogues containing *N*-5-butyl-arylamides (**22a–c**) displayed full agonist activity. These functional groups have been used by a number of laboratories to make highly D₃R-selective antagonists and low efficacy partial agonists.⁹ On the basis of modeling derived from the D₃R crystal structure, an extended aryl SP attached to a PP, such as the D₂R/D₃R partial agonist 2,3-dichlorophenylpiperazine via a butylamide linker, results in compounds in which the PP binds in the OBS and the SP binds in an SBP.^{32,33} Interactions between the PP and OBS have been associated with functional activity, whereas interactions between the SP and the SBP, particularly with extracellular loop 1, typically dictate subtype selectivity.^{33,48}

Under the hypothesis that **1** occupies the OBS of D₂R or D₃R in a manner similar to dopamine and the phenylpiperazine moiety of reported D₃R-selective antagonists, it is likely that the agonist activity of **22a–c** is mediated by interactions of their 5,6-dihydro-4*H*-imidazo[4,5-*l*]-quinolin-2(1*H*)-one PP within the OBS. This also provides an explanation for previously reported D₃R-selective agonists containing the 6-*N*-propyl-4,5,6,7-tetrahydro-1,3-benzothiazole-2,6-diamine of D₃R agonist pramipexole as the PP and a butyl-arylamide as the SP.^{49,50}

Structural Basis for the D₂R over D₃R Selectivity of Compound 1. To understand the structural basis of the D₂R over D₃R selectivity of compound **1**, we used molecular modeling and simulations to compare the binding modes of compound **1** in D₂R and D₃R. Our docking results showed that in both D₂R and D₃R, the protonated amine *N*-5 forms a salt bridge with the side chain of conserved Asp^{3,32}, and the aromatic moiety contacts residues Phe^{6,51}, Phe^{6,52}, and His^{6,55} of transmembrane 6 (TM6) in the OBS;⁵¹ however, the orientation of the imidazolinone moiety is ambiguous. Top-scoring docking poses in either receptor did not show a clear preference for the carbonyl O of the imidazolinone moiety to point either up toward the second extracellular loop (EL2) (“up” pose) or down toward the intracellular side of the transmembrane domain (“down” pose).

To further evaluate the orientational preference of the imidazolinone moiety, we carried out molecular dynamics (MD) simulations starting from either the “up” or the “down” pose for both D₂R and D₃R (see [Experimental Methods](#) for details). The simulations indicated that the “up” poses in D₂R and D₃R converged: the *N*-1 forms a hydrogen bond with the side chain of Ser^{5,42}, whereas the carbonyl O of the imidazolinone moiety forms a hydrogen bond with the side chain of His^{6,55} ([Figure 2a,b](#)). By contrast, the “down” poses in D₂R and D₃R showed divergent interactions with the receptors: the *N*-1 interacts with Ser193^{5,42} in D₂R, whereas it interacts with Ser196^{5,46} in D₃R instead ([Figure 2c,d](#)). By calculating the ligand–receptor binding energy using the Molecular Mechanics/Generalized Born Surface Area (MM/GBSA) approach for the frames along each MD trajectory, we found that the “down” pose has more favorable binding energy than the “up” pose in D₂R; however, the reverse preference was marginally observed in D₃R ([Figure 2e](#)). Furthermore, the “down” pose in D₂R has more favorable energy than either “up” or “down” poses in D₃R ([Figure 2e](#)), consistent with the higher affinity of compound **1** for D₂R over D₃R.

To further validate the differential binding modes of **1** in D₂R and D₃R, we carried out docking studies using the resulting models from our MD simulations (see [Experimental Methods](#)) for selected compound **1** analogues, compounds **13** and **15**. As described above, the replacement of the *N*-5-CH₃ group in **1** with an *n*-propyl group (**13**) improved binding affinities at both

D₂R and D₃R while retaining some selectivity, albeit lower than that of **1** ($K_i = 2.78$ and 25.5 nM for D₂R and D₃R, respectively; D₃R/D₂R = 9.2-fold selectivity). The *N*-*n*-propyl substitutions at positions 1 and 5 (**15**), on the other hand, improved the affinity only at D₃R but not D₂R compared to **13** ($K_i = 2.59$ and 3.39 nM for D₂R and D₃R, respectively; D₃R/D₂R = 1.3-fold selectivity), resulting in the complete loss of D₂R selectivity. Our docking results for **13**, which retains some selectivity, showed the same preference for the “up” or “down” orientation compared to **1** ([Figure 3a,b](#)). The improved affinities of **13** in both D₂R and D₃R can be attributed to the *n*-propyl group at position 5 inserting into a previously identified high affinity hydrophobic pocket at the interface of TMs 6 and 7 (Ptm67 pocket).³³ In contrast, the docking results for **15**, which loses selectivity, showed that the “up” orientation is preferred in both D₂R and D₃R, i.e., the alkylations at positions 1 and 5 cause a switch in the orientational preference of the imidazolinone moiety in D₂R ([Figure 3c,d](#)). The improved affinity of **15** compared to **13** in D₃R can be attributed to the *n*-propyl groups at positions 1 and 5, making additional interactions with the pockets at the interface of TMs 3 and 5 and the interface of TMs 2 and 3 (Ptm23 pocket).³³ The lack of change in affinity of **15** compared to **13** in D₂R is likely due to the competing effects of the unfavorable switch in the imidazolinone orientation from “down” to “up” and the favorable additional interactions formed by the *n*-propyl groups. Thus, the predicted binding poses of **13** and **15** in D₂R and D₃R establish SAR consistent with the experimental results and support the differential binding modes of their parent compound **1** in these two receptors.

We observed divergent conformations of EL2 and the extracellular portion of TMS that may contribute to the differential binding modes in D₂R and D₃R. Specifically, several divergent residues in and near EL2 and Ile203^{5,52} in D₂R relative to Gly202^{5,52} in D₃R likely modulate the proline kink (prokink) angles at Pro^{5,50} differentially,⁵² resulting in a larger distance between the extracellular tips of TMs 3 and 5 in D₂R compared to D₃R; consequently, the subcavity enclosed by EL2 and the extracellular portion of TMS accommodate the imidazolinone moiety of **1** differently in D₂R and D₃R ([Figure 2c,d](#)).

CONCLUSIONS

In the present study, we report the synthesis of parent compound **1** and a series of 1-, 5-, and 8-substituted analogues that were evaluated for binding and functional activity at D₂R and D₃R. Importantly, binding conditions—notably the use of agonist or antagonist radioligand probes—dramatically affect calculated binding affinities, especially for D₂R, in turn altering calculated receptor selectivity ratios. Relatedly, compound **1** is considerably less D₂R-selective in our binding and functional studies than previously reported.²² In this series of **1** analogues, D₃R affinity generally improved along with D₂R affinity, resulting in analogues with higher D₂R affinity but less D₂R selectivity than the parent ligand. Modifications at different positions on the parent compound template had distinct effects. For example, simple alkyl substitutions at the *N*-1 position produced analogues with reduced efficacy at D₃R and no significant subtype selectivity, suggesting that modification at this position differentially affects interactions at the OBS, which is highly homologous between D₂R and D₃R. Modification with *n*-butyl-arylamide linkers at the *N*-5 position, found in classic D₃R-selective antagonists,³⁴ was well-tolerated and resulted in

potent and relatively nonselective D₂R full agonists with improved D₂R binding affinity. This finding demonstrates that the butyl-arylamide does not universally differentiate binding at D₂R and D₃R, as has been observed in the 4-phenylpiperazine class of D₃R-selective antagonists/partial agonists, and extends our hypothesis that binding of the PP in the OBS determines how the rest of the molecule binds to the receptor, affecting both efficacy and subtype selectivity.

On the basis of molecular modeling and simulation data, **1** and the analogues described herein bind to and activate D₂R and D₃R similarly. However, amino acid sequence differences between D₂R and D₃R in two regions, EL2 and the N-terminal segment of TMS, may dictate the subtype selectivity of **1** and the analogues reported in this study. The contributions of subtle differences in the binding mode of the PP in the OBS and additional contributions of the SP to subtype selectivity and efficacy will require further investigation. Moreover, in the absence of a crystal structure of the active state of either D₂R or D₃R, more extensive SAR studies will be required in the pursuit of highly D₂R-selective agonists.

EXPERIMENTAL METHODS

Synthesis. All chemicals and solvents were purchased from chemical suppliers unless otherwise stated and used without further purification. Dry THF was freshly distilled from sodium benzophenone ketyl. All melting points were determined on a Thomas-Hoover melting point apparatus and are uncorrected. The ¹H and ¹³C NMR spectra were recorded on a Varian Mercury Plus 400 instrument. Proton chemical shifts are reported as parts per million (δ ppm) relative to tetramethylsilane (0.00 ppm) as an internal standard. Coupling constants are measured in Hz. Chemical shifts for ¹³C NMR spectra are reported as parts per million (δ ppm) relative to deuterated CHCl₃ or deuterated MeOH (CDCl₃, 77.5 ppm, CD₃OD 49.3 ppm). Infrared spectra were recorded as a neat film on NaCl plates with a PerkinElmer Spectrum RX I FT-IR system. Microanalyses were performed by Atlantic Microlab, Inc. (Norcross, GA) and agree with $\pm 0.4\%$ of calculated values. All column chromatography was performed using silica gel (Merck, 230–400 mesh, 60 Å) or preparative thin layer chromatography (silica gel, Analtech, 1000 μ m). The eluting solvent system CHCl₃/CH₃OH/NH₄OH (CMA) in the percentage indicated where NH₄OH is 1%. If not otherwise stated, all spectroscopic data and yields refer to the free base. On the basis of these analyses, all final compounds are >95% pure.

General Synthetic Procedure for 3a,b from 2a,b. A solution of 3-substituted D-phenylalanine and NaOH (1 equiv) in H₂O (NaOH/H₂O; 1 g/30 mL) and THF (phenylalanine/THF; 1 mmol/1.5 mL) was cooled to -15°C , and a solution of methyl chloroformate or benzyl chloroformate (1.3 equiv) in THF (acid chloride/THF; 4 mmol/1 mL) was added dropwise. When one-half of the acid chloride had been added, a solution of NaOH (1.5 equiv) in H₂O (NaOH/H₂O; 1 g/2 mL) was added, and the addition continued. The reaction mixture was stirred at rt for an additional 2 h after the addition was completed, and it was then acidified with 10% aq HCl solution to pH 2. The mixture was extracted twice with Et₂O, and the combined extracts were washed with brine, dried (MgSO₄), and filtered. The solvent was removed under vacuum to leave the product as a clear oil. Compound **3a** was used for the next step without purification.

(R)-2-((Methoxycarbonyl)amino)-3-(3-bromophenyl)propanoic acid (3b). Compound **3b** was prepared from **2b** (5.01 g, 20.5 mmol) in 90% (5.54 g) as a clear oil, which slowly solidified to a white solid after standing at rt. Mp $67\text{--}71^{\circ}\text{C}$. ¹H NMR (400 MHz, CDCl₃) δ 7.40 (m, 1H), 7.34 (s, 1H), 7.18 (t, $J = 8.0$ Hz, 1H), 7.11 (d, $J = 7.6$ Hz, 1H), 5.13 (d, $J = 8.0$ Hz, 1H), 4.66 (dd, $J = 6.0, 5.6$ Hz, 1H), 3.69 (s, 3H), 3.18 (dd, $J = 13.8, 6.0$ Hz, 1H), 3.06 (dd, $J = 14.0, 6.4$ Hz, 1H).

General Synthetic Procedure for 4a,b from 3a,b. To a solution of **3a,b** in CH₂Cl₂ was added an aq solution of Na₂CO₃ (0.65

eq, Na₂CO₃/H₂O (1 g/1.7 mL). Methoxyamine hydrochloride (CH₃ONH₂·HCl; 1.15 equiv) and EDC (1.1 equiv) were then added, and the resulting mixture was stirred at rt for 24 h. The mixture was diluted with THF (to dissolve the precipitate), and the layers were separated. The aq layer was extracted with 1:1 THF/Et₂O, and the combined organic extracts were washed with 10% aq HCl solution and a saturated NaHCO₃ solution successively. The organic layer was dried (MgSO₄) and concentrated to give the crude product **4a,b**.

Benzyl (R)-[1-Methoxyamino-1-oxo-3-phenylpropan-2-yl]carbamate (4a). Compound **4a** was obtained as a white solid in 69% yield (22.5 g) from **2a** (16.5 g) in 2 steps and purified by crystallization from ethyl acetate. Mp $136\text{--}140^{\circ}\text{C}$ (dec). ¹H NMR (400 MHz, CDCl₃) δ 8.51 (br s, 1H), 7.38–7.16 (m, 10H), 5.37 (br s, 1H), 5.07 (s, 2H), 4.23 (m, 1H), 3.61 (s, 3H), 3.08 (m, 2H).

Methyl (R)-[3-(3-Bromophenyl)-1-methoxyamino-1-oxopropan-2-yl]carbamate (4b). Compound **4b** was obtained as a white solid in 88% yield (5.28 g) from **3b** (5.45 g, 18.0 mmol) and purified by crystallization from ethyl acetate. Mp $143\text{--}145^{\circ}\text{C}$. ¹H NMR (400 MHz, CDCl₃) δ 9.21 (br, 1H), 7.36 (d, $J = 1.2$ Hz, 2H), 7.15 (m, 2H), 5.56 (br, 1H), 4.28 (m, 1H), 3.64 (s, 3H), 3.62 (s, 3H), 3.02 (m, 2H).

General Synthetic Procedure for 5a,b from 4a,b. A suspension of compound **4a,b** in CH₂Cl₂ (**4a,b**/CH₂Cl₂; 1 mmol/4 mL) was cooled in an ice bath, and CF₃CO₂H (2.7 equiv) was added. Bis(trifluoroacetoxy)iodobenzene (PhI(CF₃CO₂)₂; 1 equiv) was added portionwise over 10 min at 0°C , and the mixture was stirred at this temperature for 1 h. The mixture was washed with a 10% Na₂CO₃ solution and dried (MgSO₄). Solvent was removed under vacuum to give the product as an amber oil. Purification by flash column chromatography, eluting with hexane/EtOAc (1:1) gave the desired product **5a,b**.

Benzyl (R)-[1-Methoxy-2-oxo-1,2,3,4-tetrahydroquinolin-3-yl]carbamate (5a). Compound **5a** was prepared from **4a** (11.2 g, 34.2 mmol) and purified by column chromatography in 90% yield (10.2 g) as a light brown solid. Mp $59\text{--}62^{\circ}\text{C}$. IR (NaCl): 1694 cm^{-1} . ¹H NMR (400 MHz, CDCl₃) δ 7.38 (m, 5H), 7.33 (m, 1H), 7.22 (d, $J = 8.0$ Hz, 2H), 7.08 (dt, $J = 7.6, 1.2$ Hz, 1H), 5.84 (br, 1H), 5.15 (s, 2H), 4.41 (m, 1H), 3.93 (s, 3H), 3.47 (m, 1H), 2.84 (t, $J = 14.8$ Hz, 1H).

Methyl (R)-[6-Bromo-1-methoxy-2-oxo-1,2,3,4-tetrahydroquinolin-3-yl]carbamate (5b). Compound **5b** was prepared from **4b** (5.18 g, 15.7 mmol) and purified by column chromatography in 88% yield (5.57 g) as a light brown solid. Mp $97\text{--}99.5^{\circ}\text{C}$. ¹H NMR (400 MHz, CDCl₃) δ 7.45 (d, $J = 8.0$ Hz, 1H), 7.38 (s, 1H), 7.10 (d, $J = 8.0$ Hz, 1H), 5.78 (br, 1H), 4.40 (m, 1H), 3.93 (s, 3H), 3.76 (s, 3H), 3.39 (m, 1H), 2.83 (t, $J = 10.8$ Hz, 1H).

(R)-3-Amino-1-methoxy-3,4-dihydroquinolin-2(1H)-one (6a). Compound **5a** (4.00 g) was dissolved in ethanol (80 mL) in a Parr bottle, and 10% Pd/C (400 mg) was added. The mixture was hydrogenolyzed (with an initial pressure of 50 psi) until its completion (the reaction was monitored by TLC). The mixture was then filtered over Celite, and the filtrate was concentrated under vacuum to give **6a**, which was used in the next step without further purification. Mp $183\text{--}185^{\circ}\text{C}$. ¹H NMR (400 MHz, CDCl₃) δ 7.31 (m, 1H), 7.17 (d, $J = 8.4$ Hz, 2H), 7.03 (dt, $J = 7.4, 7.4$ Hz, 1H), 3.89 (s, 3H), 3.60 (dd, $J = 6.4, 6.0$ Hz, 1H), 3.06 (dd, $J = 6.4, 6.0$ Hz, 1H), 2.81 (t, $J = 14.2$ Hz, 1H), 2.04 (br s, 2H). GC-MS (EI) m/z 192 (M⁺).

General Synthetic Procedure for 7a,b from 5b or 6a. A solution or suspension of **5b** or **6a** (4 mL of THF/mmol) in THF was cooled to 0°C , and borane-methyl sulfide (BH₃·Me₂S; 10.0 M, 6 equiv) was added slowly. The mixture was allowed to warm to rt and stirred for 2.5 h. The mixture was heated to reflux for 48 h (solution) or 5 days (suspension). The resulting clear solution was then cooled to 0°C and quenched slowly with 10% HCl solution (**Caution!**: hydrogen evolution). The mixture was heated to reflux again for 1.5 h, cooled to 0°C , and basified (pH >10) with 12 N NaOH solution. The mixture was extracted twice with Et₂O, and the combined extracts were washed with brine, dried (MgSO₄), and concentrated to give a clear oil (**7b**) or a dark oil (**7a**), which was carried on to the next reaction without further purification.

(R)-1,2,3,4-Tetrahydroquinolin-3-amine (7a).²⁰ ¹H NMR (400 MHz, CDCl₃) δ 6.98 (m, 2H), 6.63 (m, 1H), 6.49 (d, $J = 10.4$ Hz,

1H), 3.83 (br, 1H), 3.36 (m, 2H), 3.03 (m, 2H), 2.78 (dd, $J = 14.8$, 6.4 Hz, 1H), 1.68 (br, 2H). GC-MS (EI) m/z 148 (M+).

(R)-6-Bromo-N-methyl-1,2,3,4-tetrahydroquinolin-3-amine (7b). GC-MS (EI) m/z 240 (M+), 242 (M+).

General Synthetic Procedure for 8a,b from 7a,b. A solution of 7a,b in toluene (0.6 mL of toluene/mmol) was stirred at $-40\text{ }^{\circ}\text{C}$ while *N*-(benzyloxycarbonyloxy)succinimide (1.15 equiv) in toluene (1.5 mL of toluene/mmol) was added slowly. The mixture was stirred at this temperature for 30 min after the addition and quenched with a 10% NaHCO_3 solution. The mixture was then allowed to warm to $0\text{ }^{\circ}\text{C}$, and MeOH was added. The resulting mixture was stirred at rt overnight and extracted with EtOAc. The combined extracts were dried (MgSO_4) and concentrated to afford the crude product, which was purified by flash column chromatography to give the desired product 8a,b.

Benzyl (R)-(1,2,3,4-Tetrahydroquinolin-3-yl)carbamate (8a). Compound 8a was prepared from 7a (410 mg, 2.77 mmol) and purified by column chromatography, eluting with hexane/ethyl acetate (2:1) as a solid in 80% yield (626 mg). Mp $76\text{--}78.5\text{ }^{\circ}\text{C}$. $^1\text{H NMR}$ (400 MHz, CDCl_3) δ 7.39–7.28 (m, 5H), 6.97 (dd, $J = 8.8$, 2.0 Hz, 2H), 6.64 (dt, $J = 8.8$, 0.8 Hz, 1H), 6.50 (dd, $J = 8.8$, 0.8 Hz, 1H), 5.16 (s, 2H), 4.57 (m, 1H), 3.30 (d, $J = 6.8$ Hz, 2H), 3.02–2.80 (m, 4H). GC-MS (EI) m/z 282 (M+).

Benzyl (R)-(6-Bromo-1,2,3,4-tetrahydroquinolin-3-yl)(methyl)carbamate (8b). Compound 8b was prepared from 5b (5.50 g, 16.7 mmol) in 2 steps and purified by column chromatography, eluting with hexane/ethyl acetate (2:1) in 64% yield (4.07 g). $^1\text{H NMR}$ (400 MHz, CDCl_3) δ 7.36–7.26 (m, 8H), 5.11 (s, 2H), 4.44 (m, 1H), 3.85 (m, 1H), 3.25 (m, 2H), 2.93–2.81 (m, 2H), 2.88 (s, 3H).

General Synthetic Procedure for 9a,b from 8a,b. A solution of 8a,b and Et_3N (3 equiv) in dry THF (4 mL THF/mmol) was added dropwise to a solution of phosgene (1.07 equiv) in THF (8 mL of THF/mmol) at $0\text{ }^{\circ}\text{C}$. After 1 h, $\text{CH}_3\text{ONH}_2\cdot\text{HCl}$ (2 equiv) and Et_3N (3 equiv) were added, and the mixture was stirred at rt for 2 days. The mixture was diluted with Et_2O and washed with H_2O and brine. The organic layer was dried (MgSO_4) and concentrated to give crude product 9a,b.

Benzyl (R)-(1-(Methoxycarbonyl)-1,2,3,4-tetrahydroquinolin-3-yl)carbamate (9a). Compound 9a was prepared from 8a (1.63 g, 6.97 mmol) and purified by column chromatography, eluting with hexane/ethyl acetate (1:2) as a solid in 74% yield (1.56 g). Mp $107\text{--}108.5\text{ }^{\circ}\text{C}$. IR (NaCl): 1694 cm^{-1} . $^1\text{H NMR}$ (400 MHz, CDCl_3) δ 7.86 (br, 1H), 7.40 (m, 1H), 7.31 (m, 5H), 7.19 (m, 1H), 7.16–7.04 (m, 2H), 5.06 (br s, 3H), 4.19 (m, 1H), 3.74 (m, 2H), 3.70 (s, 3H), 3.07 (m, 1H), 2.71 (m, 1H).

Benzyl (R)-(6-Bromo-1-(methoxycarbonyl)-1,2,3,4-tetrahydroquinolin-3-yl)(methyl)carbamate (9b). Compound 9b was prepared from 8b (3.18 g, 8.48 mmol) and purified by flash column chromatography (hexane/ethyl acetate; 1:2) as a white solid in 94% yield (3.58 g). Mp $104\text{--}106\text{ }^{\circ}\text{C}$ (dec). $^1\text{H NMR}$ (400 MHz, CDCl_3) δ 7.64 (br, 1H), 7.38–7.26 (m, 8H), 5.14 (s, 2H), 4.44 (m, 1H), 3.86 (m, 1H), 3.77–3.72 (m, 1H), 3.74 (s, 3H), 2.93–2.81 (m, 2H), 2.88 (s, 3H).

General Synthetic Procedure for 10a,b from 9a,b. A solution of 9a,b in CHCl_3 (7.5 mL CHCl_3 /mmol) was cooled to $-5\text{ }^{\circ}\text{C}$ in an ice-salt bath. $\text{PhI}(\text{CF}_3\text{CO}_2)_2$ (1.2 equiv) was added, and the mixture was stirred at -5 to $0\text{ }^{\circ}\text{C}$ for 4 h and then at rt for 2 h. The reaction mixture was washed with a 10% Na_2CO_3 solution, back-extracting the aq layer with Et_2O . The combined organic layers were dried (MgSO_4) and concentrated to give a brown oil. Purification by flash column chromatography, eluting with hexane/EtOAc (40:60) afforded the product 10a,b.

Benzyl (R)-(1-Methoxy-2-oxo-1,2,5,6-tetrahydro-4H-imidazo[4,5,1-*ij*]quinolin-5-yl)carbamate (10a). Compound 10a was prepared from 9a (6.30 g, 17.7 mmol) and purified by column chromatography as a light brown solid in 82% yield (5.17 g). Mp $70\text{--}73\text{ }^{\circ}\text{C}$ (dec). $[\alpha]_D^{24} -13.5$ (c 0.43, MeOH). $^1\text{H NMR}$ (400 MHz, CDCl_3) δ 7.35 (m, 5H), 7.03 (t, $J = 7.8$ Hz, 1H), 6.98 (d, $J = 7.6$ Hz, 1H), 6.88 (d, $J = 7.6$ Hz, 1H), 5.07 (s, 2H), 4.87 (br, 1H), 4.54 (m,

1H), 4.08 (s, 3H), 4.01 (m, 1H), 3.83 (dd, $J = 12.0$, 3.6 Hz, 1H), 3.11 (m, 1H), 2.90 (m, 1H).

Benzyl (R)-(8-Bromo-1-methoxy-2-oxo-1,2,5,6-tetrahydro-4H-imidazo[4,5,1-*ij*]quinolin-5-yl)(methyl)carbamate (10b). Compound 10b was prepared from 9b (3.40 g, 7.59 mmol) and purified by column chromatography as a light brown solid in 73% yield (2.48 g). Mp $168\text{--}170\text{ }^{\circ}\text{C}$ (dec). $^1\text{H NMR}$ (400 MHz, CDCl_3) δ 7.38 (m, 5H), 6.94 (s, 1H), 6.86 (s, 1H), 5.14 (s, 2H), 4.53 (m, 1H), 4.12 (m, 1H), 4.08 (s, 3H), 3.74 (m, 1H), 3.17 (m, 1H), 3.02–2.90 (m, 1H), 2.95 (s, 3H).

Benzyl (R)-(8-Cyano-1-methoxy-2-oxo-1,2,5,6-tetrahydro-4H-imidazo[4,5,1-*ij*]quinolin-5-yl)(methyl)carbamate (11b). To a solution of 10b (2.38 g, 5.30 mmol) in DMF (20 mL) was added $\text{Zn}(\text{CN})_2$ (1.24 g, 10.6 mmol) and $\text{Pd}(\text{PPh}_3)_4$ (0.30 g, 5 mol %) under argon. The reaction mixture was heated to $80\text{ }^{\circ}\text{C}$ overnight. DMF was removed under vacuum, and the mixture was filtered. The filtrate was diluted with H_2O and extracted 3 times with EtOAc. The combined organic layers were dried (MgSO_4) and concentrated. The residue was purified by flash column chromatography, eluting with hexane/EtOAc (40:60) to afford 11b in 63% yield (1.31 g) as a white solid. Mp $174\text{--}176\text{ }^{\circ}\text{C}$ (dec). $^1\text{H NMR}$ (400 MHz, CDCl_3) δ 7.36 (m, 5H), 7.24 (s, 1H), 7.21 (s, 1H), 5.17 (s, 2H), 4.58 (m, 1H), 4.16–4.09 (m, 1H), 4.10 (s, 3H), 3.74 (m, 1H), 3.17 (m, 1H), 3.02–2.90 (m, 1H), 2.95 (s, 3H).

General Synthetic Procedure for 12a,b from 10a, 11b. A mixture of 10a or 11b and $\text{Pd}(\text{OH})_2/\text{C}$ (20%, 4.0 g of 10a or 11b/1.0 g of catalyst) in absolute ethanol (20 mL/1.0 g of 10a or 11b) in a Parr bottle was hydrogenolyzed (50 psi). After the reaction was completed (~ 20 h, monitored by TLC), the mixture was filtered through Celite. Removal of the solvent afforded the crude product, which was purified by flash chromatography, eluting with CMA to give 12a,b.

(R)-5-Amino-5,6-dihydro-4H-imidazo[4,5,1-*ij*]quinolin-2(1H)-one (12a).²⁰ Compound 12a was prepared from 10a (6.34 g, 18 mmol) and purified by column chromatography (10% CMA) as an oil in 73% yield (2.48 g). $[\alpha]_D^{23} -16.9$ (c 0.52, MeOH). $^1\text{H NMR}$ (400 MHz, CDCl_3) δ 9.82 (br s, 1H), 7.00–6.91 (m, 2H), 6.83 (d, $J = 7.2$ Hz, 1H), 4.06 (dd, $J = 16.0$, 4.0 Hz, 1H), 3.62 (dd, $J = 12.0$, 7.2 Hz, 1H), 3.33 (m, 1H), 3.06 (dd, $J = 11.8$, 4.4 Hz, 1H), 2.71 (dd, $J = 16.0$, 6.6 Hz, 1H), 1.67 (br s, 2H). $^{13}\text{C NMR}$ (100 MHz, CDCl_3) δ 155.15, 127.56, 126.45, 120.84, 120.03, 117.72, 107.46, 51.57, 42.96, 30.89. GC-MS (EI) m/z 189 (M+). Anal. ($\text{C}_{10}\text{H}_{11}\text{N}_3\text{O}\cdot\text{H}_2\text{O}$) C, H, N.

(R)-5-(Methylamino)-2-oxo-1,2,5,6-tetrahydro-4H-imidazo[4,5,1-*ij*]quinolin-8-carbonitrile (12b). Compound 12b was prepared from 11b (1.00 g, 2.64 mmol) and purified by column chromatography (10% CMA) as an oil in 85% yield (0.49 g). $^1\text{H NMR}$ (400 MHz, CDCl_3) δ 7.22 (s, 1H), 7.21 (s, 1H), 3.98 (ddd, $J = 12.4$, 8.0, 0.8 Hz, 1H), 3.71 (dd, $J = 12.4$, 6.4 Hz, 1H), 3.28 (m, 1H), 3.06 (dd, $J = 16.0$, 4.0 Hz, 1H), 2.80 (dd, $J = 16.0$, 7.2 Hz, 1H), 2.53 (s, 3H). $^{13}\text{C NMR}$ (100 MHz, CDCl_3) δ 150.09, 125.99, 125.29, 124.49, 119.51, 118.35, 108.49, 104.72, 52.40, 42.70, 34.06, 30.39. GC-MS (EI) m/z 228 (M+). Anal. ($\text{C}_{12}\text{H}_{12}\text{N}_4\text{O}\cdot 1/4\text{H}_2\text{O}$) C, H, N.

(R)-5-(Propylamino)-5,6-dihydro-4H-imidazo[4,5,1-*ij*]quinolin-2(1H)-one (13).²⁰ To a solution of 12a (230 mg, 1.20 mmol) in THF (5 mL) was added propionaldehyde (84 mg, 1.44 mmol), $\text{NaBH}(\text{OAc})_3$ (381 mg, 1.80 mmol), and a catalytic amount of HOAc (2–3 drops), and the mixture was stirred at rt overnight. The reaction mixture was basified with a minimum volume of saturated Na_2CO_3 solution. H_2O and solvent were then removed under vacuum. The residue was further dried under high vacuum, and CHCl_3 (20 mL) was added. The mixture was filtered, and the solid was washed with CHCl_3 (3×20 mL). The filtrate was concentrated to give crude product 13, which was purified by column chromatography, eluting with 15% CMA to afford pure product (200 mg) in 71% yield. $[\alpha]_D^{24} -15.6$ (c 1.1, MeOH). $^1\text{H NMR}$ (400 MHz, CDCl_3) δ 9.94 (br s, 1H), 7.00–6.91 (m, 2H), 6.86 (d, $J = 7.2$ Hz, 1H), 4.10 (dd, $J = 12.0$, 4.0 Hz, 1H), 3.62 (dd, $J = 12.0$, 7.2 Hz, 1H), 3.33 (m, 1H), 3.06 (dd, $J = 16.0$, 4.4 Hz, 1H), 2.82–2.66 (m, 3H), 1.67 (br s, 1H), 1.51 (m, 2H), 0.93 (t, $J = 7.6$ Hz, 3H). $^{13}\text{C NMR}$ (100 MHz, CDCl_3) δ 155.15, 127.28, 126.24, 121.52, 119.86, 117.54, 107.54, 51.57, 49.25, 43.25, 31.35,

23.37, 11.70. GC-MS (EI) m/z 231 (M+). Anal. (C₁₃H₁₇N₃O·1/2H₂O) C, H, N.

(*R*)-5-(Dipropylamino)-5,6-dihydro-4*H*-imidazo[4,5,1-*ij*]quinolin-2(1*H*)-one (**14a**).²⁰ Benzyl chloroformate (639 mg, 3.75 mmol) in dry THF (2 mL) was added dropwise at 0 °C under argon to a solution of **13** (787 mg, 3.41 mmol) and Et₃N (1.38 g, 13.6 mmol) in dry THF (10 mL). The reaction was warmed to rt for 3 h after the addition. The mixture was diluted with H₂O, and the two layers were separated. The aqueous layer was extracted with CHCl₃. The combined organic layers were dried (MgSO₄) and concentrated. The residue was purified by column chromatography (eluting with CHCl₃/MeOH; 93:7) to afford benzyl (*R*)-2-oxo-5-(propylamino)-5,6-dihydro-4*H*-imidazo[4,5,1-*ij*]quinoline-1(2*H*)-carboxylate (853 mg, 69%). ¹H NMR (400 MHz, CDCl₃) δ 7.55–7.50 (m, 3H), 7.42–7.31 (m, 3H), 7.01 (t, *J* = 7.8 Hz, 2H), 6.96 (m, 1H), 5.48 (s, 2H), 3.99 (ddd, *J* = 12.8, 4.0, 1.2 Hz, 1H), 3.60 (dd, *J* = 12.8, 7.0 Hz, 1H), 3.28 (m, 1H), 3.04 (dd, *J* = 16.0, 4.0 Hz, 1H), 2.80–2.61 (m, 3H), 1.56–1.43 (m, 2H), 0.91 (t, *J* = 7.2 Hz, 3H). To a solution of this CBz-protected intermediate (683 mg, 1.87 mmol) in DMF (10 mL) were added K₂CO₃ (516 mg, 3.74 mmol) and *n*-PrBr (460 mg, 3.74 mmol), and the mixture was heated to 65 °C and stirred overnight. The mixture was then cooled to rt and filtered. The filtrate was concentrated. The residue was diluted with H₂O (10 mL) and extracted with EtOAc (3 × 20 mL). The combined organic layers were dried (MgSO₄) and concentrated. The residue was purified by column chromatography (eluting with CHCl₃/MeOH; 93:7) to provide benzyl (*R*)-5-(dipropylamino)-2-oxo-5,6-dihydro-4*H*-imidazo[4,5,1-*ij*]quinoline-1(2*H*)-carboxylate (356 mg) in 46% yield. ¹H NMR (400 MHz, CDCl₃) δ 7.54–7.50 (m, 3H), 7.42–7.31 (m, 3H), 7.02–6.94 (m, 2H), 5.48 (s, 2H), 4.14 (ddd, *J* = 12.0, 4.8, 0.8 Hz, 1H), 3.41 (t, *J* = 11.8 Hz, 1H), 3.24 (m, 1H), 2.96–2.81 (m, 2H), 2.60–2.44 (m, 4H), 1.52–1.40 (m, 4H), 0.89 (t, *J* = 7.2 Hz, 6H). This intermediate (330 mg, 0.81 mmol) was dissolved in EtOH (10 mL) in a Parr bottle, and Pd/C (10%, 50 mg) was added. The mixture was hydrogenolyzed at an initial pressure of 50 psi for 5 h. The mixture was then filtered over Celite. The filtrate was concentrated, and the residue was purified by column chromatography (eluting with 10% CMA) to give pure product **14a** (179 mg) in 81% yield. [α]_D²⁵ –4.25 (*c* 0.6, CHCl₃). ¹H NMR (400 MHz, CDCl₃) δ 10.20 (br, 1H), 6.98–6.91 (m, 2H), 6.85 (d, *J* = 6.8 Hz, 1H), 4.18 (ddd, *J* = 11.6, 4.0, 0.8 Hz, 1H), 3.46 (t, *J* = 11.4 Hz, 1H), 3.31 (m, 1H), 2.97–2.83 (m, 2H), 2.60–2.46 (m, 4H), 1.45 (m, 4H), 0.90 (t, *J* = 7.2 Hz, 6H). ¹³C NMR (100 MHz, CDCl₃) δ 155.26, 127.33, 126.27, 121.32, 119.66, 119.11, 107.35, 54.74, 52.81, 40.39, 26.74, 22.30, 11.69. GC-MS (EI) m/z 273 (M+). Anal. (C₁₆H₂₃N₃O·0.25 H₂O) C, H, N.

(*R*)-5-(Propylamino)-1-propyl-5,6-dihydro-4*H*-imidazo[4,5,1-*ij*]quinolin-2(1*H*)-one (**14b**). Compound **13** (60 mg, 0.26 mmol) was dissolved in DMF (2 mL), and to the solution was added 1-bromopropane (62 mg, 0.52 mmol) and K₂CO₃ (72 mg, 0.52 mmol). The mixture was heated to 40 °C for 48 h. The mixture was filtered after cooling to rt, and the filtrate was concentrated under vacuum. The residue was purified by preparative TLC, eluting with 5% CMA to afford **14b** (55 mg, 78%) as an oil. [α]_D²⁴ –14.4 (*c* 0.55, MeOH). ¹H NMR (400 MHz, CDCl₃) δ 6.98 (dd, *J* = 8.0, 7.6 Hz, 1H), 6.85 (dd, *J* = 7.6, 0.8 Hz, 1H), 6.82 (d, *J* = 8.0 Hz, 1H), 4.10 (ddd, *J* = 12.0, 4.4, 1.2 Hz, 1H), 3.82 (m, 2H), 3.55 (dd, *J* = 12.0, 8.0 Hz, 1H), 3.28 (m, 1H), 3.05 (dd, *J* = 15.6, 4.4 Hz, 1H), 2.72 (m, 3H), 1.78 (m, 2H), 1.50 (m, 2H), 0.97 (t, *J* = 7.6 Hz, 3H), 0.92 (t, *J* = 7.6 Hz, 3H); ¹³C NMR (100 MHz, CDCl₃) δ 153.57, 127.82, 126.24, 120.98, 119.55, 117.44, 105.63, 51.61, 49.29, 43.53, 42.93, 31.70, 23.44, 21.97, 11.68, 11.36. GC-MS (EI) m/z 273 (M+). Anal. (C₁₆H₂₃N₃O·1/4H₂O) C, H, N.

(*R*)-5-[Methyl(propyl)amino]-5,6-dihydro-4*H*-imidazo[4,5,1-*ij*]quinolin-2(1*H*)-one (**14c**). Compound **14c** was synthesized from **1** and 1-bromopropane in 73% yield using the same procedure as for **14b**. [α]_D²⁵ –6.6 (*c* 0.29, MeOH). ¹H NMR (400 MHz, CDCl₃) δ 10.0 (s, 1H), 6.94 (m, 2H), 6.85 (d, *J* = 7.2 Hz, 1H), 4.22 (ddd, *J* = 12.0, 4.4, 1.2 Hz, 1H), 3.53 (dd, *J* = 12.0, 6.6 Hz, 1H), 3.11 (m, 1H), 2.95 (m, 2H), 2.57 (m, 2H), 2.42 (s, 3H), 1.54 (m, 2H), 0.91 (t, *J* = 7.6 Hz, 3H). ¹³C NMR (100 MHz, CDCl₃) δ 155.06, 127.35, 126.12, 121.39, 119.69, 118.63, 107.35, 57.40, 56.11, 39.98, 38.22, 27.10, 20.93, 11.70. GC-MS (EI) m/z 245 (M+). Anal. (C₁₄H₁₉N₃O·1/2H₂O) C, H, N.

(*R*)-5-(Dipropylamino)-1-propyl-5,6-dihydro-4*H*-imidazo[4,5,1-*ij*]quinolin-2(1*H*)-one (**15**). To the solution of **13** (52 mg, 0.23 mmol) in DMF (2 mL) was added 1-bromopropane (138 mg, 1.13 mmol) and K₂CO₃ (128 mg, 0.92 mmol). The mixture was heated to 65 °C overnight. The mixture was then filtered after cooling to rt, and the filtrate was concentrated under vacuum. The residue was purified by preparative TLC, eluting with 5% CMA to afford **15** (53 mg, 76%). [α]_D²⁵ –1.4 (*c* 0.70, MeOH). ¹H NMR (400 MHz, CDCl₃) δ 6.97 (dd, *J* = 7.6, 7.2 Hz, 1H), 6.85 (dd, *J* = 7.2, 0.8 Hz, 1H), 6.81 (d, *J* = 7.6 Hz, 1H), 4.17 (ddd, *J* = 11.6, 4.2, 0.8 Hz, 1H), 3.82 (t, *J* = 7.4 Hz, 2H), 3.45 (t, *J* = 11.6 Hz, 1H), 3.29 (m, 1H), 2.90 (m, 2H), 2.53 (m, 4H), 1.78 (m, 2H), 1.62 (br s, 1H), 1.45 (m, 2H), 0.97 (t, *J* = 7.6 Hz, 3H), 0.89 (t, *J* = 7.6 Hz, 6H). ¹³C NMR (100 MHz, CDCl₃) δ 153.58, 127.78, 126.28, 120.76, 119.43, 118.96, 105.38, 54.65, 52.81, 42.91, 40.47, 27.02, 22.30, 21.96, 11.68, 11.35. GC-MS (EI) m/z 315 (M+). Anal. (C₁₉H₂₉N₃O) C, H, N.

Benzyl (*R*)-Methyl(2-oxo-1,2,5,6-tetrahydro-4*H*-imidazo[4,5,1-*ij*]quinolin-5-yl)carbamate (**16**). *N*-(Benzoyloxycarbonyloxy)succinimide (386 mg, 1.55 mmol) solution in THF (10 mL) was added dropwise to the solution of **1** (300 mg, 1.47 mmol) in dry THF (10 mL) at –40 °C under an argon atmosphere. The reaction mixture was slowly warmed to rt and stirred overnight. The reaction mixture was then quenched with 10% sat. NaHCO₃ solution (20 mL) and extracted with EtOAc (3 × 10 mL). The organic layers were combined, dried, concentrated, and purified by column chromatography using 60% EtOAc/hexanes as eluent to provide 498 mg (91%) of oily material. ¹H NMR (400 MHz, CDCl₃) δ 10.23 (br, 1H), 7.36 (m, 5H), 6.95 (m, 2H), 6.84 (d, *J* = 7.8 Hz, 1H), 5.18 (s, 2H), 4.65 (m, 1H), 4.12 (dd, *J* = 11.6, 4.8 Hz, 1H), 3.71 (m, 1H), 3.13 (dd, *J* = 15.6, 11.2 Hz, 1H), 2.86 (s, 3H), 3.00–2.84 (m, 1H).

Benzyl (*R*)-Methyl(2-oxo-1-propyl-1,2,5,6-tetrahydro-4*H*-imidazo[4,5,1-*ij*]quinolin-5-yl)carbamate (**17a**). 1-Bromopropane (90 mg, 0.73 mmol) was added to the reaction mixture of **16** (122 mg, 0.36 mmol) and K₂CO₃ (504 mg, 3.66 mmol) in acetone (5 mL) and stirred at reflux for 20 h. The reaction mixture was filtered, concentrated, and purified using flash chromatography with 10% acetone/CHCl₃ as eluent to provide 138 mg (93%) of **17a**. [α]_D²⁴ +41.4 (*c* 0.58, MeOH). ¹H NMR (400 MHz, CDCl₃) δ 7.36 (br, 5H), 6.99 (ddd, *J* = 7.6, 7.2, 0.8 Hz, 1H), 6.84 (m, 2H), 5.18 (s, 2H), 4.65 (br, 1H), 4.13 (dd, *J* = 12.0, 4.8 Hz, 1H), 3.82 (t, *J* = 7.2 Hz, 2H), 3.73 (m, 1H), 3.14 (dd, *J* = 15.6, 7.2 Hz, 1H), 2.94 (m, 4H), 1.78 (m, 2H), 0.97 (dt, *J* = 7.6, 0.8 Hz, 3H).

Benzyl (*R*)-Methyl(2-oxo-1-butyl-1,2,5,6-tetrahydro-4*H*-imidazo[4,5,1-*ij*]quinolin-5-yl)carbamate (**17b**). NaH (60% in mineral oil, 30 mg, 0.75 mmol) was washed with hexane (3 × 1 mL) and then suspended in dry THF. To this suspension was added **16** (168 mg, 0.5 mmol) in dry THF, and the mixture was stirred at rt for 30 min. 1-Bromobutane (137 mg, 1.0 mmol) was added, and the mixture was stirred at rt overnight. The mixture was quenched with H₂O, extracted with CHCl₃, dried (MgSO₄), and concentrated. The residue was purified by column chromatography, eluting with hexane/ethyl acetate (1:1) to afford 115 mg (68%) of **17b**. ¹H NMR (400 MHz, CDCl₃) δ 7.33 (br, 5H), 6.97 (m, 1H), 6.83 (m, 2H), 5.18 (s, 2H), 4.63 (br, 1H), 4.13 (dd, *J* = 12.0, 4.4 Hz, 1H), 3.85 (t, *J* = 7.6 Hz, 2H), 3.74 (m, 1H), 3.12 (dd, *J* = 15.6, 7.6 Hz, 1H), 2.93 (m, 4H), 1.74 (m, 2H), 1.40 (m, 2H), 0.95 (t, *J* = 7.6 Hz, 3H).

(*R*)-5-(Methylamino)-1-propyl-5,6-dihydro-4*H*-imidazo[4,5,1-*ij*]quinolin-2(1*H*)-one (**18a**). Compound **17a** (100 mg, 0.26 mmol) and Pd/C (10%, 20 mg) in absolute EtOH (5 mL) was hydrogenolyzed (50 psi) for 5 h. TLC showed that the reaction was complete. The mixture was filtered over Celite. The filtrate was concentrated, and the residue was purified by preparative TLC, eluting with 5% CMA to provide 58 mg (90%) of **18a**. [α]_D²⁵ –12.9 (*c* 1.00, MeOH). ¹H NMR (400 MHz, CDCl₃) δ 6.98 (dd, *J* = 7.6, 7.6 Hz, 1H), 6.85 (dd, *J* = 7.6, 0.8 Hz, 1H), 6.82 (dd, *J* = 7.6, 0.8 Hz, 1H), 4.06 (ddd, *J* = 12.0, 4.0, 0.8 Hz, 1H), 3.82 (m, 2H), 3.64 (dd, *J* = 12.0, 6.8 Hz, 1H), 3.23 (m, 1H), 3.07 (dd, *J* = 16.0, 4.0 Hz, 1H), 2.78 (dd, *J* = 16.0, 7.2 Hz, 1H), 2.54 (s, 3H), 1.77 (m, 2H), 0.97 (t, *J* = 7.2 Hz, 3H). ¹³C NMR (100 MHz, CDCl₃) δ 153.61, 127.83, 126.13, 121.06, 119.62, 117.13, 105.72,

53.30, 42.96, 42.84, 34.06, 31.11, 21.97, 11.37. GC-MS (EI) m/z 245 (M⁺). Anal. (C₁₄H₁₉N₃O·1/4H₂O) C, H, N.

(*R*)-5-(Methylamino)-1-butyl-5,6-dihydro-4*H*-imidazo[4,5,1-*ij*]-quinolin-2(1*H*)-one (**18b**). Compound **18b** was synthesized from **17b** in 92% yield using the same procedure as for **18a**. [α]_D²⁵ -15.9 (*c* 0.58, MeOH). ¹H NMR (400 MHz, CDCl₃) δ 6.98 (dd, *J* = 8.0, 7.6 Hz, 1H), 6.85 (dd, *J* = 7.6, 0.8 Hz, 1H), 6.82 (d, *J* = 8.0 Hz, 1H), 4.06 (ddd, *J* = 12.0, 4.0, 1.2 Hz, 1H), 3.85 (m, 2H), 3.63 (dd, *J* = 12.0, 7.2 Hz, 1H), 3.22 (m, 1H), 3.06 (dd, *J* = 16.0, 4.2 Hz, 1H), 2.79 (dd, *J* = 16.0, 7.2 Hz, 1H), 2.54 (s, 3H), 1.73 (m, 2H), 1.40 (m, 2H), 0.95 (t, *J* = 7.6 Hz, 3H). ¹³C NMR (100 MHz, CDCl₃) δ 153.57, 127.78, 126.15, 121.04, 119.60, 117.17, 105.69, 53.30, 42.88, 41.10, 34.11, 31.16, 30.74, 20.09, 13.72. GC-MS (EI) m/z 259 (M⁺). Anal. (C₁₅H₂₁N₃O·3/4H₂O) C, H, N.

N-(4-Hydroxybutyl)-9*H*-fluorene-2-carboxamide (**20c**). Thionyl chloride (SOCl₂, 2 mL/mmol) was added to fluorene-2-carboxylic acid (2.32 g, 11.03 mmol).⁵³ The solution was stirred at reflux for 3 h and concentrated in vacuo. Residual SOCl₂ was removed by azeotropic distillation in dry benzene. The resulting solid was dissolved in CHCl₃ (5 mL). To a stirred solution of the 1-amino-4-butanol (0.98 g, 11.0 mmol) in CHCl₃ (20 mL) and 0.5 M aq sodium hydroxide (8 mL) cooled to 0 °C was added the acid chloride solution dropwise. The solution was stirred vigorously for 3 h at rt. The organic layer was separated, dried with Na₂SO₄, and concentrated in vacuo. The crude product (2.77 g, 89%) was used in the next step without purification.

N-(4-Bromobutyl)-9*H*-fluorene-2-carboxamide (**21c**). To a suspension of compound **20c** (1.50 g, 5.33 mmol) in acetonitrile were added triphenylphosphine (2.80 g, 10.7 mmol) and carbon tetrabromide (3.54 g, 10.7 mmol). The yellow solution was stirred overnight at rt. Acetonitrile was evaporated, and the product was purified by column chromatography using 25% EtOAc/hexanes as eluent to give 0.46 g (25%) of **21c**. ¹H NMR (400 MHz, CDCl₃) δ 7.97 (s, 1H), 7.83–7.76 (m, 3H), 7.58 (d, *J* = 7.6 Hz, 1H), 7.43–7.34 (m, 2H), 6.22 (br s, 1H), 3.94 (s, 2H), 3.56–3.47 (m, 4H), 2.03–1.96 (m, 2H), 1.86–1.79 (m, 2H). ¹³C NMR (100 MHz, CDCl₃) δ 167.99, 145.10, 144.16, 143.65, 140.80, 132.94, 127.84, 127.16, 125.79, 125.37, 123.95, 120.73, 119.90, 39.32, 37.05, 33.49, 30.23, 28.59.

(*R*)-*N*-(4-(Methyl(2-oxo-1,2,5,6-tetrahydro-4*H*-imidazo[4,5,1-*ij*]-quinolin-5-yl)amino)butyl)benzofuran-2-carboxamide (**22a**). To a solution of **1** (247 mg, 1.22 mmol) in DMF (5 mL) were added **21a** (360 mg, 1.22 mmol) and K₂CO₃ (503 mg, 3.64 mmol), and the mixture was heated for 3 h at 60–65 °C. The solvent was evaporated, and the product was purified by column chromatography using 1% MeOH/CH₂Cl₂ as eluent to give 79 mg (16%) of **22a**. Mp 77–78 °C. [α]_D²⁵ +10.66 (*c* 0.075, MeOH). ¹H NMR (400 MHz, CDCl₃) δ 10.31 (s, 1H), 7.64 (d, *J* = 7.6 Hz, 1H), 7.46–7.15 (m, 5H), 6.96–6.81 (m, 3H), 4.19 (dd, *J* = 11.8, 0.8 Hz, 1H), 3.57–3.47 (m, 3H), 3.26–3.19 (m, 1H), 2.98–2.88 (m, 2H), 2.67–2.59 (m, 2H), 2.40 (s, 3H), 1.74–1.70 (m, 2H), 1.65–1.60 (m, 2H). ¹³C NMR (100 MHz, CDCl₃) δ 159.02, 155.11, 154.72, 149.00, 127.70, 127.34, 126.77, 126.26, 123.67, 122.73, 121.49, 119.73, 118.44, 111.67, 110.27, 107.48, 57.48, 53.55, 39.92, 39.34, 38.19, 27.32, 26.86, 25.29. Anal. (C₂₄H₂₆N₄O₃·3H₂O) for C, H, N.

(*R*)-*N*-(4-(Methyl(2-oxo-2,4,5,6-tetrahydro-1*H*-imidazo[4,5,1-*ij*]-quinolin-5-yl)amino)butyl)-1*H*-indole-2-carboxamide (**22b**). The same procedure employed for **22a** was used for **22a** (400 mg, 1.36 mmol). The product was eluted with 2% MeOH/CH₂Cl₂ as eluent then repurified by column chromatography using 65% acetone/CHCl₃ to give 115 mg (20%) of **22b**. Mp 130–131 °C. [α]_D²⁵ +8.57 (*c* 0.075, MeOH). ¹H NMR (400 MHz, CDCl₃) δ 10.37 (s, 1H), 10.18 (s, 1H), 7.53 (d, *J* = 8.4 Hz, 1H), 7.42 (d, *J* = 8.0 Hz, 1H), 7.19 (t, *J* = 8.0 Hz, 1H), 7.06–7.02 (m, 2H), 6.92–6.83 (m, 3H), 6.76 (d, *J* = 6.8 Hz, 1H), 4.08 (dd, *J* = 11.8, 4.0 Hz, 1H), 3.48–3.41 (m, 3H), 3.10–3.03 (m, 1H), 2.86–2.74 (m, 2H), 2.53–2.41 (m, 2H), 2.27 (s, 3H), 1.61–1.56 (m, 2H), 1.52–1.47 (m, 2H). ¹³C NMR (100 MHz, CDCl₃) δ 162.26, 155.16, 136.72, 131.14, 127.67, 127.41, 126.21, 124.29, 121.90, 121.56, 120.49, 119.84, 118.57, 112.27, 107.46, 102.65, 57.34, 53.56, 40.25, 39.66, 38.18, 27.34, 26.73, 25.14. Anal. (C₂₄H₂₇N₃O₂·4H₂O) for C, H, N.

(*R*)-*N*-(4-(Methyl(2-oxo-1,2,5,6-tetrahydro-4*H*-imidazo[4,5,1-*ij*]-quinolin-5-yl)amino)butyl)-9*H*-fluorene-2-carboxamide (**22c**). The same procedure employed for **22c** was used for **22a** (561 mg, 1.63 mmol). The product was eluted with 3% MeOH/CH₂Cl₂ as eluent and then repurified by column chromatography using 65% acetone/CHCl₃ to give 184 mg (24%) of **22c**. Mp 103–104 °C. [α]_D²⁵ +8.69 (*c* 0.115, MeOH). ¹H NMR (400 MHz, CDCl₃) δ 10.51 (s, 1H), 7.94 (s, 1H), 7.79–7.23 (m, 7H), 7.14–7.11 (m, 1H), 6.89–6.72 (m, 3H), 4.05 (dd, *J* = 11.6, 4.0 Hz), 3.75 (s, 2H), 3.45 (dd, *J* = 12.4, 6.2 Hz), 3.88–3.33 (m, 1H), 3.10–3.03 (m, 1H), 2.84–2.70 (m, 2H), 2.57–2.45 (m, 2H), 2.27 (s, 3H), 1.66–1.60 (m, 2H), 1.55–1.50 (m, 2H). ¹³C NMR (100 MHz, CDCl₃) δ 168.05, 154.97, 144.50, 143.88, 143.21, 140.55, 133.07, 127.46, 127.16, 126.83, 126.19, 125.82, 125.05, 123.86, 121.35, 120.37, 119.56, 119.46, 118.27, 107.35, 57.28, 53.49, 39.93 (d, *J* = 10.3 Hz), 37.97, 36.74, 30.89, 27.21, 26.51, 25.19. Anal. (C₂₉H₃₀N₄O₂·3H₂O) C, H, N.

Radioligand Binding Studies. Radioligand binding assays were conducted similarly to methods previously described.^{12,54–56} Briefly, HEK293 cells were stably transfected with either human D₂R or human D₃R in our laboratory. These cells were grown in a 50:50 mix of DMEM and Ham's F12 culture media, supplemented with 20 mM HEPES, 2 mM L-glutamine, 0.1 mM nonessential amino acids, 1× antibiotic/antimycotic, 10% heat-inactivated fetal bovine serum, and 200 µg/mL of hygromycin (Life Technologies, Grand Island, NY) and stored in an incubator at 37 °C and 5% CO₂. Upon reaching 80–90% confluence, cells were harvested using premixed Earle's Balanced Salt Solution (EBSS) without calcium and with 5 µM EDTA (Life Technologies) and centrifuged at 3000 rpm for 10 min at 21 °C. The supernatant was removed, and the pellet was resuspended in 10 mL of hypotonic lysis buffer (5 mM MgCl₂, 5 mM Tris, pH 7.4 at 4 °C) and centrifuged at 20,000 rpm for 30 min at 4 °C. The pellet was then resuspended in fresh binding buffer. A Bradford protein assay (Bio-Rad, Hercules, CA) was used to determine the protein concentration, and membranes were diluted to 500 µg/mL. For [³H]N-methylspiperone binding studies, the binding buffer (EBSS with calcium) was made from 8.7 g/L of Earle's Balanced Salts without phenol red (US Biological, Salem, MA) and 2.2 g/L of sodium bicarbonate at pH 7.4; 500 µg/mL membranes were stored at -80 °C for later use. For [³H]7-OH-DPAT binding studies, membranes were harvested fresh; the binding buffer was made from 50 mM Tris, 10 mM MgCl₂, and 1 mM EDTA at pH 7.4.

Test compounds were freshly dissolved the day of the assay in 30% DMSO and 70% H₂O to a stock concentration of 1 mM or 100 µM. For assisting the solubilization of free-base compounds, 10 µL of glacial HOAc was added (in place of 10 µL final H₂O volume) along with 100% DMSO initially; the solution was briefly sonicated, and then the solution was brought up to 1 mM or 100 µM final concentration by adding H₂O. Each test compound was then diluted into 13 half-log serial dilutions using 30% DMSO vehicle; the final test concentrations ranged from 100 µM to 10 pM.

Membranes were diluted in fresh binding buffer to a 10× concentration: the final concentration of membranes was 10 µg total protein for [³H]N-methylspiperone binding at D₂R or D₃R, and 40 or 20 µg total protein for [³H]7-OH-DPAT binding at D₂R or D₃R, respectively. Radioligands were diluted in binding buffer to a final concentration of 0.4 nM ([³H]N-methylspiperone, PerkinElmer), 1.0 nM ([³H]7-OH-DPAT, ARC, St. Louis, MO) for D₂R, or 0.5 nM ([³H]7-OH-DPAT) for D₃R. Radioligand competition binding experiments were conducted for 60 min at rt in glass tubes containing 300 µL of fresh appropriate binding buffer containing with 0.2 mM sodium metabisulfite, 50 µL of diluted test compound, 100 µL of membranes ([³H]N-methylspiperone: 10 µg of total protein for D₂R or D₃R; [³H]7-OH-DPAT: 40 or 20 µg total protein for D₂R or D₃R, respectively), and 50 µL of radioligand for a final reaction volume of 500 µL diluted in binding buffer ([³H]N-methylspiperone: 0.4 nM final concentration, PerkinElmer, Waltham, MA; [³H]7-OH-DPAT: 1.0 and 0.5 nM final concentration for hD₂ and hD₃, respectively, ARC, St. Louis, MO). Nonspecific binding was determined in the presence of 10 µM butaclamol (Sigma-Aldrich, St. Louis, MO), and total binding was determined with 30% DMSO vehicle. All compound

dilution concentrations were run in triplicate. The reaction was incubated for 1 h at rt. The reactions were terminated by filtration through Whatman GF/B filters, presoaked for 1 h in 0.5% polyethylenimine, using a Brandel R48 filtering manifold (Brandel Instruments, Gaithersburg, MD), and washed. The filters were washed 3 times with 3 mL/wash of ice-cold binding buffer. Filters were transferred to scintillation vials and incubated with 3 mL of CytoScint liquid scintillation cocktail (MP Biomedicals, Solon, OH), and vials were counted using a PerkinElmer Tri-Carb 2910 TR liquid scintillation counter (Waltham, MA).

For both radioligands, one- and two-site models were compared in GraphPad Prism (GraphPad Software, San Diego, CA). One-site binding models were preferred over two-site binding models in an extra sum-of-squares F test; thus, individual IC_{50} values were determined for each compound via nonlinear regression using only a one-site competition model of dose–response curves in GraphPad Prism. Each IC_{50} value was converted to K_i values using the Cheng–Prusoff equation;⁵⁷ K_d values for [³H]N-methylspiperone (D₂R: 0.133 nM, D₃R: 0.265 nM) and [³H]7-OH-DPAT (D₂R: 2.24 nM, D₃R: 1.30 nM) were determined via separate saturation binding curves. Reported K_i values were determined from at least three independent experiments and are reported as mean ± SEM.

BRET-Based G_o BRET Assay. The BRET-based G_o activation assay was described previously.³³ Briefly, HEK293T cells were transiently transfected with pcDNA3.1 vectors carrying D₂R or D₃R, $G_{\alpha A}$ fused to *Renilla luciferase* 8 (Rluc8) within in α -helical domain, $G\beta_1$ fused to V1 (the N-terminal split of mVenus; residues 1–155) at its N-terminus, and $G\gamma_2$ fused to V2 (the C-terminal split of mVenus; residues 156–240) using polyethylenimine (Polysciences, Inc.). Transfected cells were maintained in culture with DMEM (GIBCO) supplemented with 10% FBS, and transfection media was replaced with fresh media after ~24 h. Experiments were performed ~48 h after transfection.

Transfected cells were then washed, harvested, and resuspended in PBS supplemented with 5 mM glucose and distributed in 96-well black/white plates (Wallac, PerkinElmer Life and Analytical Sciences). Cells were then incubated with coelenterazine H (5 μ M) (Dalton Pharma Services), and after 8 min, compounds were added with final concentrations ranging from 10 pM to 100 μ M. After 2 min, the BRET¹ signal was measured using a Pherastar FS (BMG Labtech) and was calculated as the ratio of the light emitted by mVenus (510–540 nm) over that emitted by RLuc8 (485 nm). Data were normalized to vehicle (0%) and dopamine (100%), and nonlinear regression analysis was performed using the sigmoidal dose–response function in GraphPad Prism to generate EC_{50} values. Data are expressed as a percentage of the maximum dopamine-stimulated response as mean ± SEM.

Mitogenesis Assays. Chinese hamster ovary (CHOp) cells expressing the human D₂Rs or D₃Rs were maintained in α -MEM with 10% FBS, 0.05% pen-strep, and 400 μ g/mL of G418. To measure D₂ receptor-mediated stimulation of mitogenesis, CHOp-D₂ cells were seeded in 96-well plates at a concentration of 5,000 cells/well. The cells were incubated at 37 °C in α -MEM with 10% FBS. After 48–72 h, the cells were rinsed twice with serum-free α -MEM and incubated for 24 h at 37 °C. Serial dilutions of test compounds were made in serum-free α -MEM using a Biomek robotics workstation. For agonists, the medium was removed and replaced with 100 μ L of test compound in serum-free α -MEM. After another 24 h incubation at 37 °C, 0.25 μ Ci of [³H]thymidine in α -MEM supplemented with 10% FCS was added to each well, and the plates were further incubated for 2 h at 37 °C. The cells were trypsinized by the addition of a 10× trypsin solution (1% trypsin in calcium–magnesium-free phosphate-buffered saline); cells were filtered, and radioactivity in cells was determined by scintillation spectrometry.

Identical methods were used to measure [³H]thymidine incorporation in CHOp-D₃ cells, except that cells were incubated with agonists for 16 h before the assay was terminated. Time-response curves indicated that incubation times longer than 16 h resulted in increased background and agonist EC_{50} values (i.e., decreased potency) in CHOp-D₃ cells (data not shown).

Data were normalized to dopamine (100%), and nonlinear regression analysis was performed using the sigmoidal dose–response function in GraphPad Prism to generate EC_{50} values. Data are expressed as a percentage of the maximum dopamine-stimulated response as mean ± SEM.

Molecular Modeling and Simulations. The binding modes of compound **1** in D₂R and D₃R were predicted by computational docking and molecular dynamics (MD) simulations. The ligand was docked to equilibrated models of D₂R and D₃R, which were built based on the D₃R crystal structure.^{32,33,48} The N-terminal segment was predicted de novo, and a truncated poly-Gly segment was replaced for ICL3. Docking was performed using an induced-fit docking protocol in the Schrödinger software (release 2013–3; Schrödinger, LLC: New York, NY). For both “up” and “down” orientations of the imidazolinone moiety, the best IFDScore docking pose was selected to perform the MD simulations. The binding modes of **13** and **15** in D₂R and D₃R were predicted by docking to the representative frames from the MD simulations of **1** in D₂R and D₃R.

The MD simulations were performed in the explicit water–POPC lipid bilayer solvent environment using Desmond Molecular Dynamics System (version 3.8; D. E. Shaw Research, New York, NY) with the CHARMM36 protein force field,^{58–60} the CHARMM36 lipid force field,⁶¹ and TIP3P water model. The ligand parameters were obtained from the GAAMP server⁶² with the initial force field based on CGenFF with ParamChem.⁶³ The protonation state of compound **1** at pH 7.0 was predicted by the Epik program in the Schrödinger software. The system charges were neutralized, and a solvent concentration of 0.15 M NaCl was added. The Na⁺ binding site at the highly conserved Asp²⁵⁰ is known to collapse upon receptor activation.⁶⁴ Because compound **1** is an agonist, the active-state-like conformation of the receptor was modeled without a Na⁺ ion bound at this site. The system was initially minimized and equilibrated with restraints on the ligand heavy atoms and protein backbone atoms followed by a production stage of 600 ns with all atoms unrestrained. For D₂R, a second set of trajectories (600 ns for each pose) was collected and reached convergence with the first set.

The MM/GBSA ligand–receptor binding energy was calculated using CHARMM⁶⁵ (version c36a2) with the GBSW implicit solvent model.⁶⁶ For each frame being considered, the protein and ligand components were extracted and then minimized with restraints on all heavy atoms except for the side chains within 4 Å of the ligand before the energies were calculated.

■ ASSOCIATED CONTENT

📄 Supporting Information

The Supporting Information is available free of charge on the ACS Publications website at DOI: 10.1021/acs.jmedchem.5b01612.

Elemental analysis results (PDF)

■ AUTHOR INFORMATION

Corresponding Author

*Phone: (443)-740-2887. Fax: (443)-740-2111. E-mail: anewman@intra.nida.nih.gov.

Present Address

^vT.M.K.: Department of Chemistry and Biochemistry and Department of Biomedical and Translational Sciences, College of Science and Mathematics, Rowan University, 201 Mullica Hill Road, Glassboro, NJ 08028

Author Contributions

^oM.-F.Z. and T.M.K. contributed equally to this work.

Notes

The authors declare no competing financial interest.

■ ACKNOWLEDGMENTS

Support for this research was provided by the National Institute on Drug Abuse–Intramural Research Program (A.H.N., M.-F.Z., V.K., T.M.K., A.B., C.B., C.S., L.S., and M.M.) and National Institute of Neurological Disorders and Stroke–Intramural Research Program (R.B.F. and D.R.S.). Support for J.A.J. and P.D. was provided by K05 DA022413 and R01 MH054137. Support for A.J. was provided by a National Institute on Drug Abuse/Department of Veterans Affairs Interagency Agreement, by VA Merit Review and Senior Research Career Scientist Programs, and by the Methamphetamine Abuse Research Center (P50 DA018165). The authors thank Dr. Robert Luedtke for earlier in vitro binding experiments on a subset of these analogues. This work utilized the computational resources of the NIH HPC Biowulf cluster (<http://hpc.nih.gov>).

■ ABBREVIATIONS USED

D₂R, dopamine D₂ receptor; D₃R, dopamine D₃ receptor; GPCR, G protein-coupled receptor; OBS, orthosteric binding site; PP, primary pharmacophore; SBP, secondary receptor binding pocket; SP, secondary pharmacophore; SAR, structure–activity relationship; CBz, carbobenzoxy; IA, inactive; NT, not tested; CMA, CHCl₃/CH₃OH/NH₄OH; MD, molecular dynamics; CHOp, Chinese hamster ovary

■ REFERENCES

- (1) Beaulieu, J. M.; Gainetdinov, R. R. The physiology, signaling, and pharmacology of dopamine receptors. *Pharmacol. Rev.* **2011**, *63*, 182–217.
- (2) Madras, B. K. History of the discovery of the antipsychotic dopamine D₂ receptor: a basis for the dopamine hypothesis of schizophrenia. *J. Hist. Neurosci.* **2013**, *22*, 62–78.
- (3) Seeman, P. Targeting the dopamine D₂ receptor in schizophrenia. *Expert Opin. Ther. Targets* **2006**, *10*, 515–531.
- (4) Lako, I. M.; van den Heuvel, E. R.; Knegeting, H.; Bruggeman, R.; Taxis, K. Estimating dopamine D(2) receptor occupancy for doses of 8 antipsychotics: a meta-analysis. *J. Clin. Psychopharmacol.* **2013**, *33*, 675–681.
- (5) Ferrari-Toninelli, G.; Bonini, S. A.; Cenini, G.; Maccarinelli, G.; Grilli, M.; Uberti, D.; Memo, M. Dopamine receptor agonists for protection and repair in Parkinson's disease. *Curr. Top. Med. Chem.* **2008**, *8*, 1089–1099.
- (6) Murray, A. M.; Ryoo, H. L.; Gurevich, E.; Joyce, J. N. Localization of dopamine D₃ receptors to mesolimbic and D₂ receptors to mesostriatal regions of human forebrain. *Proc. Natl. Acad. Sci. U. S. A.* **1994**, *91*, 11271–11275.
- (7) Vallone, D.; Picetti, R.; Borrelli, E. Structure and function of dopamine receptors. *Neurosci. Biobehav. Rev.* **2000**, *24*, 125–132.
- (8) Heidbreder, C. A.; Newman, A. H. Current perspectives on selective dopamine D(3) receptor antagonists as pharmacotherapeutics for addictions and related disorders. *Ann. N. Y. Acad. Sci.* **2010**, *1187*, 4–34.
- (9) Keck, T. M.; Burzynski, C.; Shi, L.; Newman, A. H. Beyond small-molecule SAR: using the dopamine D₃ receptor crystal structure to guide drug design. *Adv. Pharmacol.* **2014**, *69*, 267–300.
- (10) Newman, A. H.; Blaylock, B. L.; Nader, M. A.; Bergman, J.; Sibley, D. R.; Skolnick, P. Medication discovery for addiction: translating the dopamine D₃ receptor hypothesis. *Biochem. Pharmacol.* **2012**, *84*, 882–890.
- (11) Khaled, M. A.; Pushparaj, A.; Di Ciano, P.; Diaz, J.; Le Foll, B. Dopamine D₃ receptors in the basolateral amygdala and the lateral habenula modulate cue-induced reinstatement of nicotine seeking. *Neuropsychopharmacology* **2014**, *39*, 3049–3058.
- (12) Keck, T. M.; John, W. S.; Czoty, P. W.; Nader, M. A.; Newman, A. H. Identifying medication targets for psychostimulant addiction:

Unraveling the dopamine D₃ receptor hypothesis. *J. Med. Chem.* **2015**, *58*, 5361–5380.

- (13) Higley, A. E.; Spiller, K.; Grundt, P.; Newman, A. H.; Kiefer, S. W.; Xi, Z. X.; Gardner, E. L. PG01037, a novel dopamine D₃ receptor antagonist, inhibits the effects of methamphetamine in rats. *J. Psychopharmacol.* **2011**, *25*, 263–273.

- (14) Spiller, K.; Xi, Z. X.; Peng, X. Q.; Newman, A. H.; Ashby, C. R., Jr.; Heidbreder, C.; Gaal, J.; Gardner, E. L. The selective dopamine D₃ receptor antagonists SB-277011A and NGB 2904 and the putative partial D₃ receptor agonist BP-897 attenuate methamphetamine-enhanced brain stimulation reward in rats. *Psychopharmacology (Berl.)* **2008**, *196*, 533–542.

- (15) Micheli, F. Recent advances in the development of dopamine D₃ receptor antagonists: a medicinal chemistry perspective. *Chem-MedChem* **2011**, *6*, 1152–1162.

- (16) Lober, S.; Hubner, H.; Tschammer, N.; Gmeiner, P. Recent advances in the search for D₃- and D₄-selective drugs: probes, models and candidates. *Trends Pharmacol. Sci.* **2011**, *32*, 148–157.

- (17) Enguehard-Gueiffier, C.; Gueiffier, A. Recent progress in medicinal chemistry of D₄ agonists. *Curr. Med. Chem.* **2006**, *13*, 2981–2993.

- (18) Heier, R. F.; Dolak, L. A.; Duncan, J. N.; Hyslop, D. K.; Lipton, M. F.; Martin, I. J.; Mauragis, M. A.; Piercey, M. F.; Nichols, N. F.; Schreur, P. J.; Smith, M. W.; Moon, M. W. Synthesis and biological activities of (R)-5,6-dihydro-N,N-dimethyl-4H-imidazo[4,5,1-ij]-quinolin-5-amine and its metabolites. *J. Med. Chem.* **1997**, *40*, 639–646.

- (19) Sethy, V. H.; Ellerbrock, B. R.; Wu, H. U-95666E: a potential anti-parkinsonian drug with anxiolytic activity. *Prog. Neuro-Psychopharmacol. Biol. Psychiatry* **1997**, *21*, 873–883.

- (20) Moon, M. W.; Morris, J. K.; Heier, R. F.; Chidester, C. G.; Hoffmann, W. E.; Piercey, M. F.; Althaus, J. S.; Von Voigtlander, P. F.; Evans, D. L.; Figur, L. M.; Lahti, R. A. Dopaminergic and serotonergic activities of imidazoquinolinones and related compounds. *J. Med. Chem.* **1992**, *35*, 1076–1092.

- (21) Moon, M. W.; Morris, J. K.; Heier, R. F.; Hsi, R. S.; Manis, M. O.; Royer, M. E.; Walters, R. R.; Lawson, C. F.; Smith, M. W.; Lahti, R. A.; Piercey, M. F.; Sethy, V. H. Medicinal chemistry of imidazoquinolinone dopamine receptor agonists. *Drug Des. Discovery* **1993**, *9*, 313–322.

- (22) McCall, R. B.; Lookingland, K. J.; Bedard, P. J.; Huff, R. M. Sumanrole, a highly dopamine D₂-selective receptor agonist: in vitro and in vivo pharmacological characterization and efficacy in animal models of Parkinson's disease. *J. Pharmacol. Exp. Ther.* **2005**, *314*, 1248–1256.

- (23) Collins, G. T.; Jackson, J. A.; Koek, W.; France, C. P. Effects of dopamine D(2)-like receptor agonists in mice trained to discriminate cocaine from saline: influence of feeding condition. *Eur. J. Pharmacol.* **2014**, *729*, 123–131.

- (24) Collins, G. T.; Newman, A. H.; Grundt, P.; Rice, K. C.; Husbands, S. M.; Chauvignac, C.; Chen, J.; Wang, S.; Woods, J. H. Yawning and hypothermia in rats: effects of dopamine D₃ and D₂ agonists and antagonists. *Psychopharmacology (Berl.)* **2007**, *193*, 159–170.

- (25) Achat-Mendes, C.; Grundt, P.; Cao, J.; Platt, D. M.; Newman, A. H.; Spealman, R. D. Dopamine D₃ and D₂ receptor mechanisms in the abuse-related behavioral effects of cocaine: studies with preferential antagonists in squirrel monkeys. *J. Pharmacol. Exp. Ther.* **2010**, *334*, 556–565.

- (26) Tremblay, P. L.; Bedard, M. A.; Levesque, M.; Chebli, M.; Parent, M.; Courtemanche, R.; Blanchet, P. J. Motor sequence learning in primate: role of the D₂ receptor in movement chunking during consolidation. *Behav. Brain Res.* **2009**, *198*, 231–239.

- (27) de Paulis, T. Sumanrole Pharmacology. *Curr. Opin. Investig. Drugs* **2003**, *4*, 77–82.

- (28) Barone, P.; Lamb, J.; Ellis, A.; Clarke, Z. Sumanrole versus placebo or ropinirole for the adjunctive treatment of patients with advanced Parkinson's disease. *Mov. Disord.* **2007**, *22*, 483–489.

- (29) Garcia-Borreguero, D.; Winkelman, J.; Adams, A.; Ellis, A.; Morris, M.; Lamb, J.; Layton, G.; Versavel, M.; Sumanriole in, R. L. S. S. G. Efficacy and tolerability of sumanirole in restless legs syndrome: a phase II, randomized, double-blind, placebo-controlled, dose-response study. *Sleep Med.* **2007**, *8*, 119–127.
- (30) Singer, C.; Lamb, J.; Ellis, A.; Layton, G. A comparison of sumanirole versus placebo or ropinirole for the treatment of patients with early Parkinson's disease. *Mov. Disord.* **2007**, *22*, 476–482.
- (31) Zintzaras, E.; Kitsios, G. D.; Papatheasiou, A. A.; Konitsiotis, S.; Miligkos, M.; Rodopoulou, P.; Hadjigeorgiou, G. M. Randomized trials of dopamine agonists in restless legs syndrome: a systematic review, quality assessment, and meta-analysis. *Clin. Ther.* **2010**, *32*, 221–237.
- (32) Chien, E. Y.; Liu, W.; Zhao, Q.; Katritch, V.; Han, G. W.; Hanson, M. A.; Shi, L.; Newman, A. H.; Javitch, J. A.; Cherezov, V.; Stevens, R. C. Structure of the human dopamine D3 receptor in complex with a D2/D3 selective antagonist. *Science* **2010**, *330*, 1091–1095.
- (33) Newman, A. H.; Beuming, T.; Banala, A. K.; Donthamsetti, P.; Pongetti, K.; LaBounty, A.; Levy, B.; Cao, J.; Michino, M.; Luedtke, R. R.; Javitch, J. A.; Shi, L. Molecular determinants of selectivity and efficacy at the dopamine D3 receptor. *J. Med. Chem.* **2012**, *55*, 6689–6699.
- (34) Furman, C. A.; Roof, R. A.; Moritz, A. E.; Miller, B. N.; Doyle, T. B.; Free, R. B.; Banala, A. K.; Paul, N. M.; Kumar, V.; Sibley, C. D.; Newman, A. H.; Sibley, D. R. Investigation of the binding and functional properties of extended length D3 dopamine receptor-selective antagonists. *Eur. Neuropsychopharmacol.* **2015**, *25*, 1448–1461.
- (35) Jean-Gérard, L.; Collet, S.; Guingant, A.; Macé, F.; Dentel, H.; Ngo, A. N.; Evain, M. A New synthesis of (R)-(-)-sumanirole (PNU-95666E). *Synlett* **2010**, *2010*, 1473–1476.
- (36) Wuts, P. G. M.; Gu, R. L.; Northuis, J. M.; Kwan, T. A.; Beck, D. M.; White, M. J. Development of a practical synthesis of sumanirole. *Pure Appl. Chem.* **2002**, *74*, 1359–1368.
- (37) Jean-Gérard, L.; Macé, F.; Ngo, A. N.; Pauvert, M.; Dentel, H.; Evain, M.; Collet, S.; Guingant, A. Remote control of the C-3-C-4 double-bond epoxidation of a chiral 1,2-dihydroquinoline: Application to the synthesis of (-)-(R)-sumanirole (PNU-95666E). *Eur. J. Org. Chem.* **2012**, *2012*, 4240–4248.
- (38) Romero, A. G.; Darlington, W. H.; McMillan, M. W. Synthesis of the selective D2 receptor agonist PNU-95666E from D-phenylalanine using a sequential oxidative cyclization strategy. *J. Org. Chem.* **1997**, *62*, 6582–6587.
- (39) Wuts, P. G. Synthesis of PNU-95666E. *Curr. Opin. Drug Discovery Devel.* **1999**, *2*, 557–564.
- (40) Jian, Z. G. Synthesis of stable isotope labeled PNU-95666. *J. Labelled Compd. Radiopharm.* **2004**, *47*, 609–614.
- (41) Campiani, G.; Butini, S.; Trotta, F.; Fattorusso, C.; Catalanotti, B.; Aiello, F.; Gemma, S.; Nacci, V.; Novellino, E.; Stark, J. A.; Cagnotto, A.; Fumagalli, E.; Carnovali, F.; Cervo, L.; Mennini, T. Synthesis and pharmacological evaluation of potent and highly selective D3 receptor ligands: inhibition of cocaine-seeking behavior and the role of dopamine D3/D2 receptors. *J. Med. Chem.* **2003**, *46*, 3822–3839.
- (42) Lahti, R. A.; Evans, D. L.; Figur, L. M.; Carrigan, K. J.; Moon, M. W.; Hsi, R. S. Dopamine D2 receptor binding properties of [3H]U-86170, a dopamine receptor agonist. *Eur. J. Pharmacol.* **1991**, *202*, 289–291.
- (43) Newman, A. H.; Grundt, P.; Cyriac, G.; Deschamps, J. R.; Taylor, M.; Kumar, R.; Ho, D.; Luedtke, R. R. N-(4-(4-(2,3-dichloro-2-methoxyphenyl)piperazin-1-yl)butyl)heterobiarylcarboxamides with functionalized linking chains as high affinity and enantioselective D3 receptor antagonists. *J. Med. Chem.* **2009**, *52*, 2559–2570.
- (44) Zhen, J.; Antonio, T.; Ali, S.; Neve, K. A.; Dutta, A. K.; Reith, M. E. Use of radiolabeled antagonist assays for assessing agonism at D2 and D3 dopamine receptors: comparison with functional GTPγS assays. *J. Neurosci. Methods* **2015**, *248*, 7–15.
- (45) Levant, B. The D3 dopamine receptor: neurobiology and potential clinical relevance. *Pharmacol. Rev.* **1997**, *49*, 231–252.
- (46) Vanhauwe, J. F.; Fraeyman, N.; Francken, B. J.; Luyten, W. H.; Leysen, J. E. Comparison of the ligand binding and signaling properties of human dopamine D(2) and D(3) receptors in Chinese hamster ovary cells. *J. Pharmacol. Exp. Ther.* **1999**, *290*, 908–916.
- (47) Malmberg, A.; Mohell, N. Characterization of [3H]quinpirole binding to human dopamine D2A and D3 receptors: effects of ions and guanine nucleotides. *J. Pharmacol. Exp. Ther.* **1995**, *274*, 790–797.
- (48) Michino, M.; Donthamsetti, P.; Beuming, T.; Banala, A.; Duan, L.; Roux, T.; Han, Y.; Trinquet, E.; Newman, A. H.; Javitch, J. A.; Shi, L. A single glycine in extracellular loop 1 is the critical determinant for pharmacological specificity of dopamine D2 and D3 receptors. *Mol. Pharmacol.* **2013**, *84*, 854–864.
- (49) Johnson, M.; Antonio, T.; Reith, M. E.; Dutta, A. K. Structure-activity relationship study of N(6)-(2-(4-(1H-Indol-5-yl)piperazin-1-yl)ethyl)-N(6)-propyl-4,5,6,7-tetrahydrobenzo[d]thiazole-2,6-diamine analogues: development of highly selective D3 dopamine receptor agonists along with a highly potent D2/D3 agonist and their pharmacological characterization. *J. Med. Chem.* **2012**, *55*, 5826–5840.
- (50) Chen, J.; Collins, G. T.; Levant, B.; Woods, J.; Deschamps, J. R.; Wang, S. CJ-1639: A potent and highly selective dopamine D3 receptor full agonist. *ACS Med. Chem. Lett.* **2011**, *2*, 620–625.
- (51) Michino, M.; Beuming, T.; Donthamsetti, P.; Newman, A. H.; Javitch, J. A.; Shi, L. What can crystal structures of aminergic receptors tell us about designing subtype-selective ligands? *Pharmacol. Rev.* **2015**, *67*, 198–213.
- (52) Ballesteros, J. A.; Shi, L.; Javitch, J. A. Structural mimicry in G protein-coupled receptors: implications of the high-resolution structure of rhodopsin for structure-function analysis of rhodopsin-like receptors. *Mol. Pharmacol.* **2001**, *60*, 1–19.
- (53) Robarge, M. J.; Husbands, S. M.; Kieltyka, A.; Brodbeck, R.; Thurkauf, A.; Newman, A. H. Design and synthesis of [(2,3-dichlorophenyl)piperazin-1-yl]alkylfluorenylcarboxamides as novel ligands selective for the dopamine D3 receptor subtype. *J. Med. Chem.* **2001**, *44*, 3175–3186.
- (54) Chun, L. S.; Free, R. B.; Doyle, T. B.; Huang, X. P.; Rankin, M. L.; Sibley, D. R. D1-D2 dopamine receptor synergy promotes calcium signaling via multiple mechanisms. *Mol. Pharmacol.* **2013**, *84*, 190–200.
- (55) Free, R. B.; Chun, L. S.; Moritz, A. E.; Miller, B. N.; Doyle, T. B.; Conroy, J. L.; Padron, A.; Meade, J. A.; Xiao, J.; Hu, X.; Dulcey, A. E.; Han, Y.; Duan, L.; Titus, S.; Bryant-Genevier, M.; Barneva, E.; Ferrer, M.; Javitch, J. A.; Beuming, T.; Shi, L.; Southall, N. T.; Marugan, J. J.; Sibley, D. R. Discovery and characterization of a G protein-biased agonist that inhibits beta-arrestin recruitment to the D2 dopamine receptor. *Mol. Pharmacol.* **2014**, *86*, 96–105.
- (56) Chen, J.; Levant, B.; Jiang, C.; Keck, T. M.; Newman, A. H.; Wang, S. Tranylcypromine substituted cis-hydroxycyclobutylphthalamides as potent and selective dopamine D(3) receptor antagonists. *J. Med. Chem.* **2014**, *57*, 4962–4968.
- (57) Cheng, Y.; Prusoff, W. H. Relationship between the inhibition constant (K_i) and the concentration of inhibitor which causes 50% inhibition (I₅₀) of an enzymatic reaction. *Biochem. Pharmacol.* **1973**, *22*, 3099–3108.
- (58) MacKerell, A. D.; Bashford, D.; Bellott, M.; Dunbrack, R. L.; Evanseck, J. D.; Field, M. J.; Fischer, S.; Gao, J.; Guo, H.; Ha, S.; Joseph-McCarthy, D.; Kuchnir, L.; Kuczera, K.; Lau, F. T.; Mattos, C.; Michnick, S.; Ngo, T.; Nguyen, D. T.; Prodhom, B.; Reiher, W. E.; Roux, B.; Schlenkrich, M.; Smith, J. C.; Stote, R.; Straub, J.; Watanabe, M.; Wiorkiewicz-Kuczera, J.; Yin, D.; Karplus, M. All-atom empirical potential for molecular modeling and dynamics studies of proteins. *J. Phys. Chem. B* **1998**, *102*, 3586–3616.
- (59) Mackerell, A. D., Jr.; Feig, M.; Brooks, C. L., 3rd Extending the treatment of backbone energetics in protein force fields: limitations of gas-phase quantum mechanics in reproducing protein conformational distributions in molecular dynamics simulations. *J. Comput. Chem.* **2004**, *25*, 1400–1415.

(60) Best, R. B.; Zhu, X.; Shim, J.; Lopes, P. E.; Mittal, J.; Feig, M.; Mackerell, A. D., Jr. Optimization of the additive CHARMM all-atom protein force field targeting improved sampling of the backbone phi, psi and side-chain chi(1) and chi(2) dihedral angles. *J. Chem. Theory Comput.* **2012**, *8*, 3257–3273.

(61) Klauda, J. B.; Venable, R. M.; Freites, J. A.; O'Connor, J. W.; Tobias, D. J.; Mondragon-Ramirez, C.; Vorobyov, I.; MacKerell, A. D., Jr.; Pastor, R. W. Update of the CHARMM all-atom additive force field for lipids: validation on six lipid types. *J. Phys. Chem. B* **2010**, *114*, 7830–7843.

(62) Huang, L.; Roux, B. Automated force field parameterization for non-polarizable and polarizable atomic models based on target data. *J. Chem. Theory Comput.* **2013**, *9*, 3543–3556.

(63) Vanommeslaeghe, K.; Hatcher, E.; Acharya, C.; Kundu, S.; Zhong, S.; Shim, J.; Darian, E.; Guvench, O.; Lopes, P.; Vorobyov, I.; Mackerell, A. D., Jr. CHARMM general force field: A force field for drug-like molecules compatible with the CHARMM all-atom additive biological force fields. *J. Comput. Chem.* **2010**, *31*, 671–690.

(64) Katritch, V.; Fenalti, G.; Abola, E. E.; Roth, B. L.; Cherezov, V.; Stevens, R. C. Allosteric sodium in class A GPCR signaling. *Trends Biochem. Sci.* **2014**, *39*, 233–244.

(65) Brooks, B. R.; Brooks, C. L., 3rd; Mackerell, A. D., Jr.; Nilsson, L.; Petrella, R. J.; Roux, B.; Won, Y.; Archontis, G.; Bartels, C.; Boresch, S.; Caflisch, A.; Caves, L.; Cui, Q.; Dinner, A. R.; Feig, M.; Fischer, S.; Gao, J.; Hodoscek, M.; Im, W.; Kuczera, K.; Lazaridis, T.; Ma, J.; Ovchinnikov, V.; Paci, E.; Pastor, R. W.; Post, C. B.; Pu, J. Z.; Schaefer, M.; Tidor, B.; Venable, R. M.; Woodcock, H. L.; Wu, X.; Yang, W.; York, D. M.; Karplus, M. CHARMM: the biomolecular simulation program. *J. Comput. Chem.* **2009**, *30*, 1545–1614.

(66) Im, W.; Lee, M. S.; Brooks, C. L., 3rd Generalized born model with a simple smoothing function. *J. Comput. Chem.* **2003**, *24*, 1691–1702.